NFATc1 in CD4$^+$ T cells and CD11c$^+$ dendritic cells drives T_H2-mediated eosinophilic inflammation in allergic asthma

Zuqin Yang, MSc,[a] Susanne Krammer, RPh,[a] Hannah Mitländer,[a] Janina C. Grund,[a] Sabine Zirlik, MD,[b] Stefan Wirtz, PhD,[b] Manfred Rauh, PhD,[c] Atefeh Sadeghi Shermeh, MSc,[d] and Susetta Finotto, PhD[a,e,f] *Erlangen, Germany*

GRAPHICAL ABSTRACT

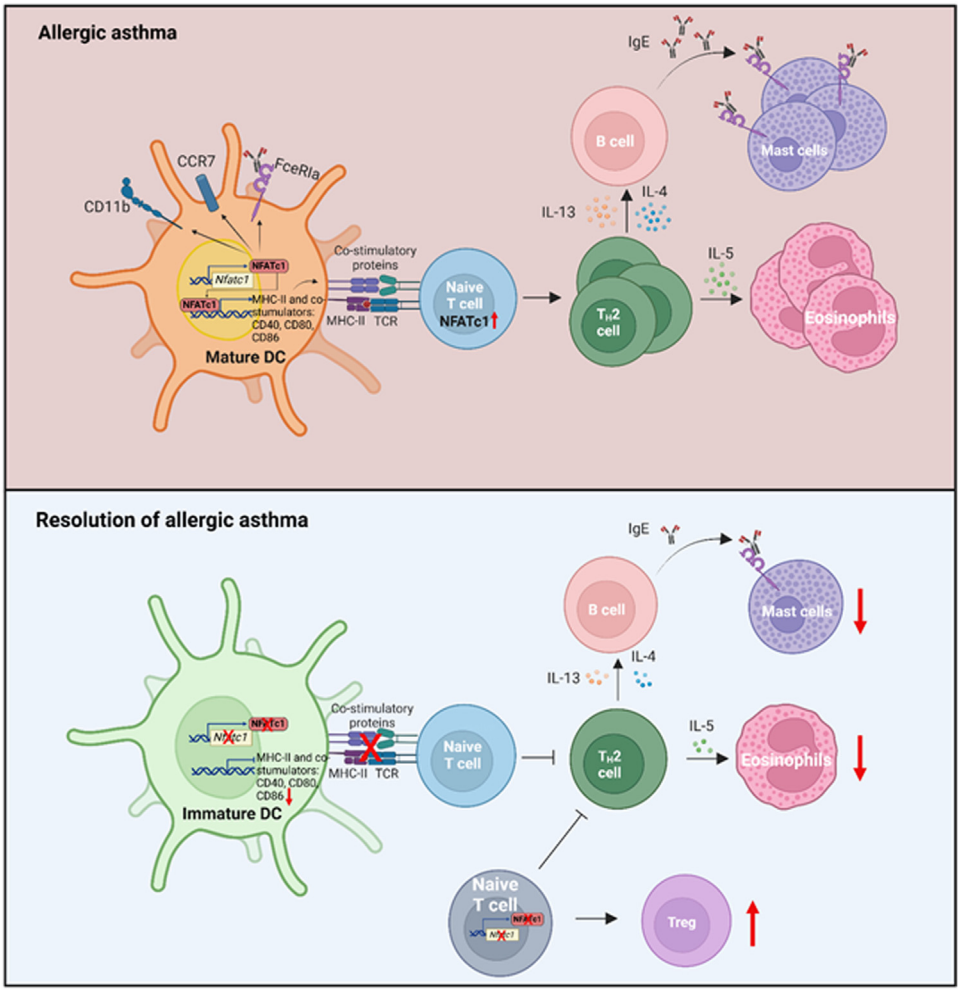

From [a]the Department of Molecular Pneumology, [b]the Department of Internal Medicine 1, [c]the Department of Pediatrics, and [d]the Department of Immune Modulation, Friedrich-Alexander-University Erlangen-Nürnberg, Universitätsklinikum Erlangen, [e]the Bavarian Cancer Research Center, and [f]the Comprehensive Cancer Center Erlangen-EMN, Erlangen.

Received for publication June 27, 2024; revised August 30, 2024; accepted for publication September 3, 2024.

Available online October 18, 2024.

Corresponding author: Susetta Finotto, PhD, Universitätsklinikum Erlangen, Department of Molecular Pneumology, Hartmannstraße 14, 91052 Erlangen, Germany. E-mail: susetta.finotto@uk-erlangen.de.

The CrossMark symbol notifies online readers when updates have been made to the article such as errata or minor corrections

2772-8293

https://doi.org/10.1016/j.jacig.2024.100355

Background: Asthma, a chronic lung disease, is a significant public health problem worldwide. It is marked by increased T_H2 response resulting in eosinophil accumulation. The pathophysiology of asthma involves various cell types, including epithelial cells, dendritic cells (DCs), innate lymphoid cells, B cells, and effector cells. Nuclear factor of activated T cells, cytoplasmic 1 (NFATc1), a critical transcription factor for immune regulation, is known for its role in T cells and, more recently, in myeloid cells. However, the specific contributions of NFATc1 in T cells and DCs in the context of asthma are not well understood.

Objective: We explored NFATc1's role in T cells and DCs in modulating T_H2 immune responses within the pathophysiology of allergic asthma.

Methods: We induced asthma in mice lacking *Nfatc1* in $CD4^+$ T cells or $CD11c^+$ DCs using house dust mite, thereby enabling investigation into NFATc1's role in both cell types in experimental allergic asthma. Additionally, we examined NFATc1 expression in these cell types and its correlation with blood eosinophil levels in an adult asthma cohort.

Results: In a house dust mite–induced asthma model, we found that *Nfatc1* deficiency either in $CD4^+$ T cells or $CD11c^+$ DCs resulted in reduced T_H2-driven eosinophilic inflammation, IgE levels, and mast cell presence in the lung of asthmatic mice. *Nfatc1*'s absence in $CD4^+$ T cells directly hampered T_H2 cell polarization and functionality, whereas in $CD11c^+$ DCs, it affected DC differentiation and maturation, thereby weakening T-cell priming, proliferation, and subsequent T_H2 differentiation. Correspondingly, translational research indicated significant correlations between $CD4^+NFATc1^+$ and $CD11c^+NFATc1^+$ cell populations and eosinophil levels in asthmatic patients, but not in healthy controls.

Conclusion: NFATc1 in T cells and DCs modulates T_H2-mediated eosinophilic inflammation in allergic asthma, thus offering insight into asthma pathogenesis and identifying NFATc1 as a potential target for therapeutic intervention. (J Allergy Clin Immunol Global 2025;4:100355.)

Key words: *NFATc1, dendritic cells, T cells, T_H2, eosinophils, allergic asthma*

Abbreviations used

ACK: Ammonium–chloride–potassium
Areg: Amphiregulin
AZCRA: Investigation of the Role of Cytokines, Chemokines, and Their Receptors in the Inflammatory Process in Asthma Patients study
BAL: Bronchoalveolar lavage
BM: Bone marrow
CCR7: C-C chemokine receptor type 7
DC: Dendritic cell
FACS: Fluorescence-activated cell sorting
FcεRI: High-affinity IgE receptor
FOXP3: Forkhead box P3
GATA3: GATA-binding protein 3
HDM: House dust mite
iEOS: Inflammatory eosinophils
MHC: Major histocompatibility complex
NFAT(c1): Nuclear factor of activated T cells (cytoplasmic 1)
PBMC: Peripheral blood mononuclear cell
PBS: Phosphate-buffered saline
PCA: Principal component analysis
Pparg: Peroxisome proliferator-activated receptor γ
qPCR: Real-time quantitative PCR
rGM-CSF: Recombinant granulocyte-macrophage colony-stimulating factor
RNA-Seq: RNA sequencing
RT: Room temperature
Siglec: Sialic acid immunoglobulin-like lectin
Treg: Regulatory T

Allergic asthma is a chronic inflammatory disease of the airways that affects millions of people worldwide. In the pathogenesis of asthma, a variety of cell types, including epithelial cells, innate lymphoid cells, B cells, and various effector cells, orchestrate a complex immunologic interplay that underpins the disease's pathology.[1] Allergic asthma often arises in response to allergenic stimuli, leading to a pronounced T_H2 cell response.[1] This response is characterized by the release of cytokines such as IL-4, IL-5, and IL-13, which mediate the hallmark features of asthma, including airway hyperresponsiveness, elevated IgE synthesis, mucus overproduction, and eosinophilic inflammation.[1-4]

NFATc1, a member of the nuclear factor of activated T cells (NFAT) family, plays a pivotal role in regulating the proliferation and survival of peripheral T cells. The NFATc1 (nuclear factor of activated T cells, cytoplasmic 1) pathway is calcium and calcineurin dependent.[5,6] T-cell receptor activation triggers phosphoinositide phospholipase C γ activation and calcium signaling, leading to calmodulin-activated calcineurin, which is targeted by immunosuppressants like cyclosporin A.[6] Activated calcineurin dephosphorylates NFAT, enabling nuclear import and gene expression regulation.[5,7] NFAT interacts with the activator protein 1 transcription factor in the nucleus, influencing the transcription of various immune response genes.[8,9] The NFATc1 protein, especially its shortest isoform, NFATc1/aA, is activated in T cells through initial and subsequent stimulations. This self-regulation boosts the proliferation and functionality of T cells in response to antigens. Moreover, NFATc1/aA is vital in safeguarding T cells from swift cell death caused by activation.[10,11]

NFATc1's role in T cells indicates its potential involvement in asthma pathogenesis. Our past study revealed elevated NFATc1 level and a correlation between NFATc1 and NFAT-interacting protein 45, a transcription factor that induces IL-4, in asthmatic patients,[12,13] suggesting a role of NFATc1 in the regulation of IL-4 production in pediatric asthma. Additionally, targeted *Nfatc1* deletion in T cells altered cytokine profiles in a mouse asthma model induced by ovalbumin.[14]

However, the ovalbumin-induced asthma model's limitations due to the non-natural occurrence of ovalbumin as a human allergen point to the need for more clinically relevant research models. Recognizing this, in our study, we used a house dust mite (HDM)-induced asthmatic mouse model to explore NFATc1's role in T cells within the context of asthma. We observed that *Nfatc1* deficiency in $CD4^+$ T cells leads to reduced T_H2 cells, eosinophils, and IgE levels, with a concurrent increase in regulatory T (Treg) cells. In human asthma patients, we noted a significant association between $CD4^+NFATc1^+$ cells and elevated eosinophil levels, which was absent in nonasthmatic controls.

Additionally, considering the critical role of DCs in asthma, we extended our research to examine the impact of NFATc1 deficiency in DCs. Previous studies have indicated a broad role for NFAT in dendritic cell (DC)-mediated pathogen recognition and immune response modulation.[15-19] However, the specific mechanisms by which NFAT participates in DC signaling pathways and gene expression regulation, particularly in asthma, remain poorly understood. Our study demonstrated that *Nfatc1* deficiency in $CD11c^+$ cells impaired DC development and functionality, significantly affecting T-cell proliferation and T_H2 cell polarization, and resulting in reduced lung eosinophils and total IgE levels in asthmatic mice. This study contributes to a deeper understanding of the role of NFATc1 in both T cells and DCs in asthma, providing insights that may guide future therapeutic strategies targeting this complex immunologic disorder.

METHODS

Human cohort AZCRA study

To investigate asthma in humans, we designed a comprehensive cohort study called AZCRA (Investigation of the Role of Cytokines, Chemokines, and Their Receptors in the Inflammatory Process in Asthma Patients). This study encompassed both adult asthmatic individuals and healthy controls, all aged between 18 and 65 years. The University Hospital Erlangen, associated with the University of Erlangen-Nürnberg in Germany, provided ethical clearance for this study (approval No. 315_20B). Moreover, the study was officially registered in the German Clinical Trial Register under identifier DRKS00023843. Before the study, each participant was informed about its goals and procedures and gave informed consent. Blood samples were collected from the asthma group and the control subjects who were nonatopic, nonasthmatic, and within the study's age range. The AZCRA cohort's clinical characteristics are listed in Tables E1 and E2 in this article's Online Repository available at www.jaci-global.org.

From these blood samples, a detailed analysis of white blood cells was conducted by the central laboratory of University Hospital Erlangen. Moreover, serum was separated from whole blood using S-Monovette Serum Gel CAT tubes (Sarstedt, Nümbrecht, Germany), which help separate serum efficiently, and peripheral blood mononuclear cells (PBMCs) were extracted. These isolated cells were subjected to flow cytometry analysis.

Cell isolation and culture

Blood treated with EDTA from AZCRA subjects was measured and poured into a 50 mL Falcon tube. An equal amount of room-temperature phosphate-buffered saline (PBS) was added to this blood, followed by gentle mixing. In a new Sepmate-50 tube, a quantity of BioColl, equal to the blood volume, was prelayered. This BioColl helps separate PBMCs. The blood-PBS mixture was then carefully placed over the BioColl without mixing them. The tubes were centrifuged at 4255 rpm for 10 minutes at 20°C. We carefully removed the tubes to help keep the layers separate. The PBMC layer was collected and transferred to a new 50 mL Falcon tube. The cells were washed twice with RPMI 1640 medium to remove leftover BioColl and other particles. If red blood cells were still present, cells were washed with cold ammonium–chloride–potassium (ACK) lysis buffer. This buffer (NH_4Cl, $KHCO_3$, and Na_2EDTA mixed in deionized water with a pH of 7.2-7.4) was used to break them down. The cells in the ACK lysis buffer were then immediately centrifuged. The final cell pellet was resuspended in a complete culture medium based on RPMI 1640 (Gibco; Thermo Fisher Scientific, Waltham, Mass) supplemented with 25 mmol/L HEPES (Gibco), 100 IU/mL penicillin, 100 μg/mL streptomycin, 50 μmol/L β-mercaptoethanol (Sigma-Aldrich, St Louis, Mo), 1% L-glutamine (200 mmol/L, Anprotec, Bruckberg, Germany), 1% MEM Vitamin (Sigma-Aldrich), 1% minimum essential medium (aka MEM) nonessential amino acids (Gibco), 1% sodium pyruvate (Gibco), and 10% heat-inactivated fetal bovine serum (Sigma-Aldrich). In the restimulated condition, 1 million cells in 1 mL medium were transferred into a well of a 48-well plate and treated with 2.5 μL αCD3 and 1 μL αCD28 for 4 days. After that, the cells were collected for RNA isolation or flow cytometry analysis.

Mice and genotyping

The *Nfatc1*$^{fl/fl}$, *Cd4Cre*, and *Cd11cCre* mice utilized in this study share a common genetic background of C57BL/6. These specific mouse strains—*Nfatc1*$^{fl/fl}$, *Cd4Cre,* and *Cd11cCre*—were generously provided by L. Glimcher (Weill Cornell University), Chris B. Wilson (University of Washington), and D. Dudziak's laboratory (Erlangen-Nürnberg), respectively. The conditional knockout *Nfatc1*$^{fl/fl}$ x *Cd4Cre* mice (*Cd4Cre*$^{Nfatc1\Delta/\Delta}$) or *Nfatc1*$^{fl/fl}$ x *Cd11cCre* mice (*Cd11cCre*$^{Nfatc1\Delta/\Delta}$) were generated by crossing *Nfatc1*$^{fl/fl}$ with *Cd4Cre* or *Cd11cCre* mice. The primers used for genotyping are shown in Table E3 in the Online Repository available at www.jaci-global.org.

These mice were housed in the pathogen-free animal facility of Friedrich-Alexander-University Erlangen-Nürnberg (Erlangen, Germany) and were used in experiments when they were between 6 and 8 weeks old. Both female and male mice were used in this study. All animal experiments were approved by the local ethics committees of the Regierung Unterfranken (Az 55.2.2-2532-2-633).

Mouse model of asthma

Nfatc1$^{fl/fl}$, *Nfatc1*$^{fl/fl}$ x *Cd4Cre,* or *Nfatc1*$^{fl/fl}$ x *Cd11cCre* mice aged 6-8 weeks, both female and male, were used to model asthma induction via HDM (*Dermatophagoides pteronyssinus,* Stallergenes Greer, Baar, Switzerland). The HDM-induced asthma model applied in this study was based on the protocol published by Li et al in 2021.[20] Briefly, for sensitization, we diluted 5 μL of a stock solution of HDM (2.5 mg/mL) in 195 μL of PBS and intraperitoneally injected 200 μL of the diluted solution into each mouse on days 0 and 7, resulting in a working dose of 12.5 μg. After sensitization, we administered 25 μL of 2.5 mg/mL HDM intranasally to each mouse's nose (125 μg per mouse in total) on days 14, 18, and 21 while the animal was under isoflurane anesthesia. On day 23, we conducted invasive lung function tests using the SCIREQ (SCIREQ Scientific Respiratory Equipment, Montreal, Quebec, Canada) system. The full protocol is shown in Fig 1, *A,* and Fig 2, *B*.

Invasive lung function testing

Lung function of mice was measured utilizing the advanced FlexiVent FX1 piston ventilator (SCIREQ) on day 23 of the HDM protocol. The procedure began with the careful anesthesia of the animals using 10 mg of pentobarbital sodium (Release; 300 mg/

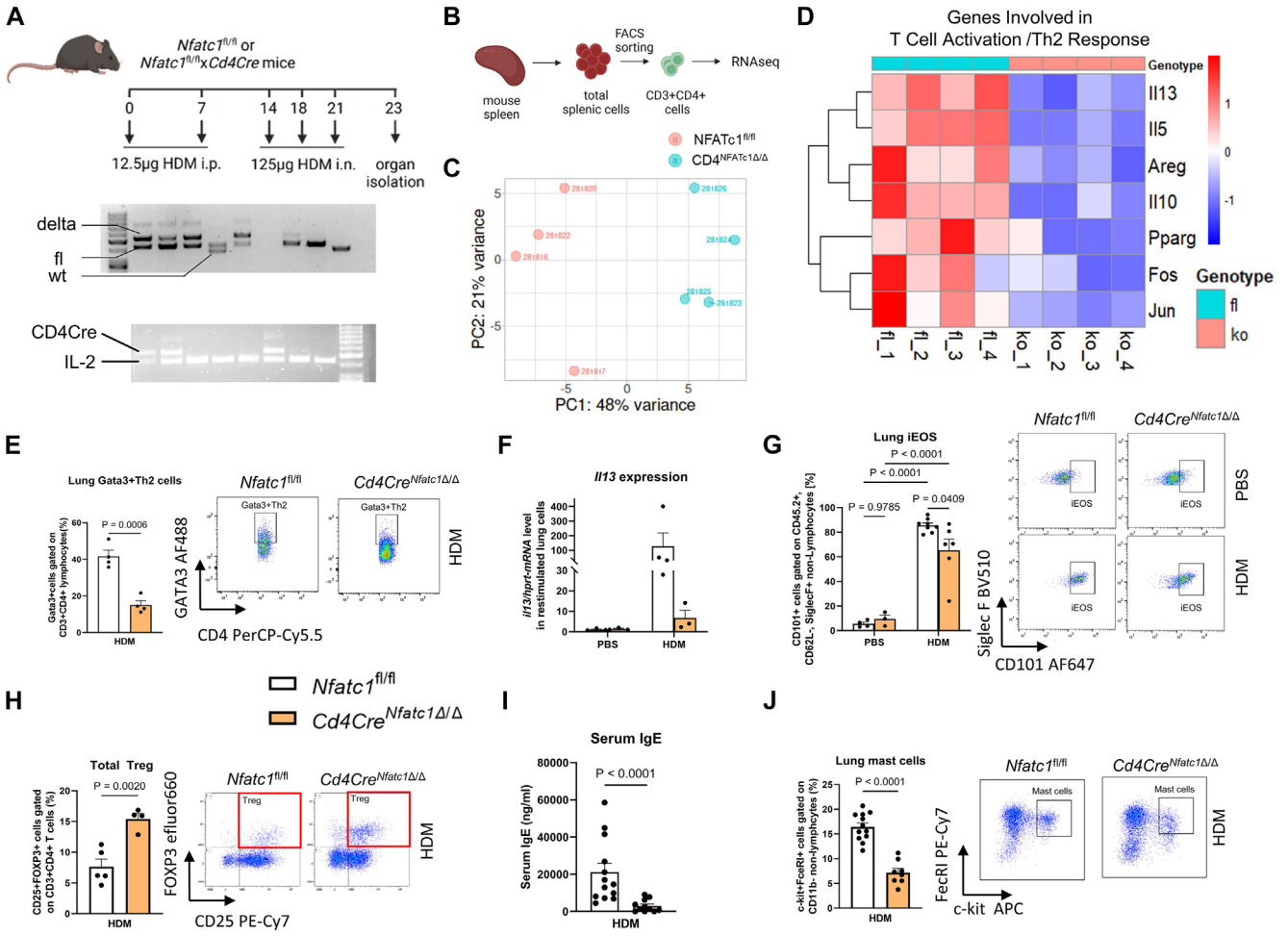

FIG 1. NFATc1 deficiency in CD4+ T cells diminished T_H2-mediated eosinophilic inflammation and allergic responses in asthma model induced by HDM. **A,** HDM-induced asthma model and genotyping in *Nfatc1*$^{fl/fl}$ and *Nfatc1*$^{fl/fl}$ x *Cd4Cre* mice. **B,** RNA-Seq experimental design for sorted splenic CD4$^+$ T cells. Schematics of *(A)* and *(B)* were created by BioRender.com. **C,** PCA plot displaying gene expression profile clustering for CD4$^+$ T cells from HDM-treated *Nfatc1*$^{fl/fl}$ *(pink)* and *Nfatc1*$^{fl/fl}$ x *Cd4Cre (light blue)* groups; numeral next to each point represents identification number of each sample. **D,** Heat map of genes associated with T-cell activation and T_H2 response in splenic CD4$^+$ T cells from *Nfatc1*$^{fl/fl}$ and *Nfatc1*$^{fl/fl}$ x *Cd4Cre* mice (n = 4/4). These genes with significant expression differences (log fold change > 1 or < −1, P_{adj} < .05) between groups. **E, G, H,** and **J,** Flow cytometry analysis of percentage of Gata3$^+$ T_H2 cells (*E*, n = 9/3/18/11), iEOS (*G*, n = 4/3/8/6), total Treg cells (*H*, n = 5/4), and mast cells (*J*, n = 12/8) in lungs of HDM-treated *Nfatc1*$^{fl/fl}$ x *Cd4Cre* and *Nfatc1*$^{fl/fl}$ mice, with representative dot plots. **F,** *Il13*–mRNA level in relative to *Hprt* in lung cells restimulated by anti-CD3/28 for 48 hours, quantified via qPCR (n = 3/3/4/3). **I,** Serum IgE levels measured by ELISA (n = 13/11). RNA-Seq data were analyzed by R software; other data were analyzed by ordinary 2-way ANOVA or unpaired 2-tailed *t* test and are presented as means ± SEMs. *Hprt,* Hypoxanthine phosphoribosyltransferase.

mL). After achievement of surgical tolerance, a meticulous tracheostomy was performed; then the animal was connected to a ventilator for mechanical ventilation via a tracheal tube. The FlexiVent FX1 system precisely recorded the respiratory system resistance value of mice, responding to progressively increasing doses of methacholine (0, 25, 50, and 100 mg/mL).

Bronchoalveolar lavage collection and cell analysis

To collect bronchoalveolar lavage (BAL) samples from mice, each mouse was first anesthetized with sodium pentobarbital. The trachea was exposed by disinfecting the neck area and removing skin and muscle. A tracheostomy provided access to the lungs. Then a cannula was inserted into the trachea, and the lungs were rinsed twice with 800 μL of Sterofundin ISO using a syringe. The collected BAL was transferred to a 15 mL tube. Cells were obtained by centrifuging the BAL samples at 1500 rpm for 5 minutes at 4°C.

For the cytospin preparation, 5×10^4 BAL cells were suspended in 100 μL PBS and transferred to slides using a centrifuge at 500 rpm for 5 minutes at room temperature (RT). After drying, the cells were stained wit a May-Grünwald/Giemsa solution (Carl Roth, Karlsruhe, Germany). For the analysis of eosinophils in BAL cells using flow cytometry, the remaining cells underwent

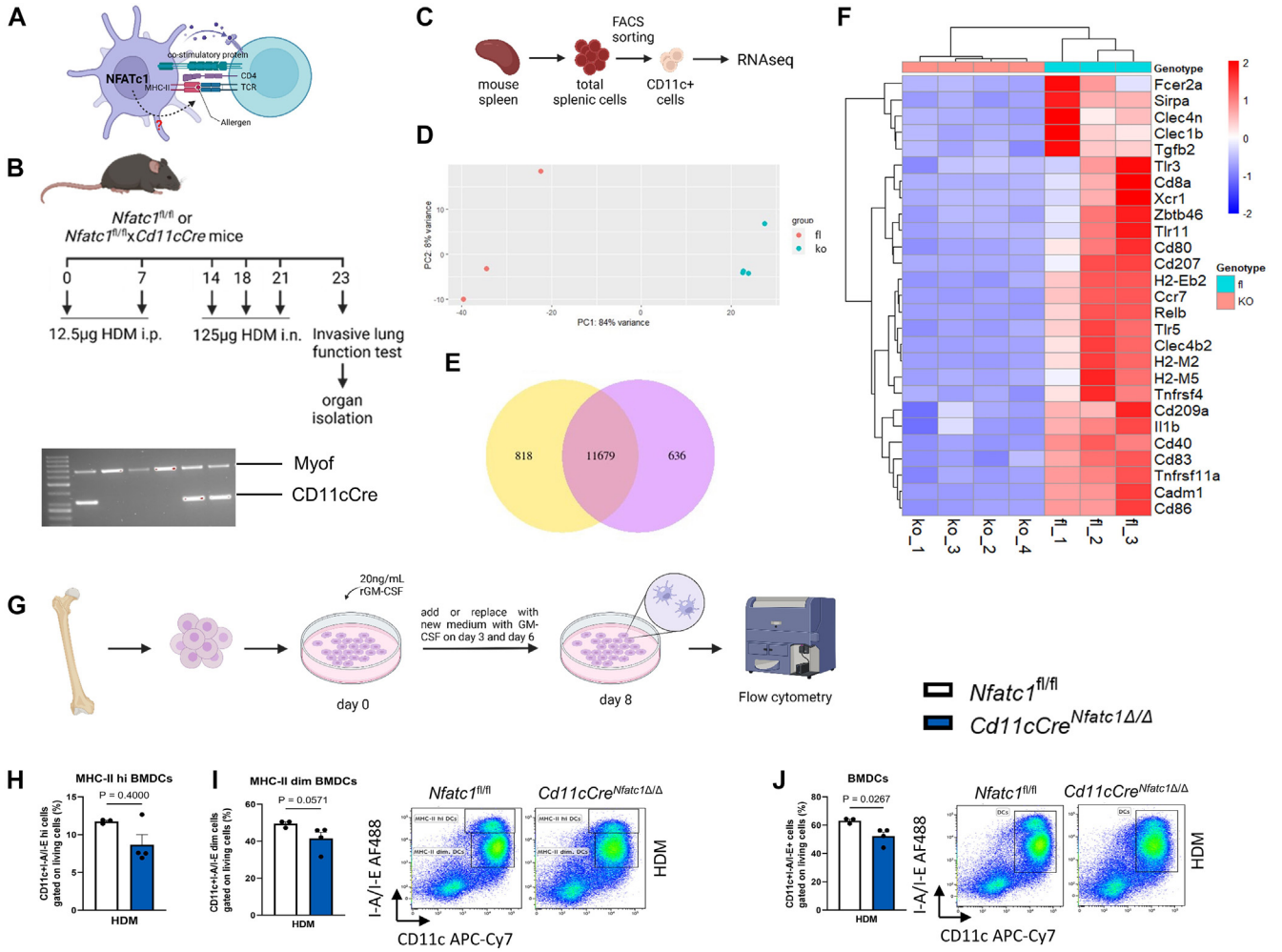

FIG 2. *Nfatc1* deficiency in CD11c cells impaired splenic and BM-derived DC differentiation. **A,** Knowledge gap of function of NFATc1 in DCs on T-cell interaction. **B,** HDM-induced asthma model and genotyping in *Nfatc1*$^{fl/fl}$ and *Nfatc1*$^{fl/fl}$ x *Cd11cCre* mice. **C,** RNA-Seq experimental design for sorted splenic CD11c^{+} cells. **D,** PCA plot displaying gene expression profile clustering for CD11c^{+} cells from HDM-treated *Nfatc1*$^{fl/fl}$ and *Nfatc1*$^{fl/fl}$ x *Cd11cCre* groups, providing insights into their gene expression differences. **E,** Venn diagram illustrating varying gene expressions in CD11c^{+} cells between HDM-treated *Nfatc1*$^{fl/fl}$ and *Nfatc1*$^{fl/fl}$ x *Cd11cCre* mice, showing both common and distinct genes. **F,** Heat map representing expression patterns of mature DC marker genes in splenic CD11c^{+} cells from HDM-treated *Nfatc1*$^{fl/fl}$ and *Nfatc1*$^{fl/fl}$ x *Cd11cCre* mice (n = 3/4). These genes with significant expression differences (log fold change > 1.5 or < −1.5, P_{adj} < .05) between groups. **G,** Schematic of experimental setup for DC differentiation using isolated BM cells cultured in presence of rGM-CSF. **H-J,** Flow cytometry analysis depicting proportions of CD11c^{+}MHC-II^{hi} DCs *(H),* CD11c^{+}MHC-II^{dim} DCs *(I),* and overall DC population (CD11c^{+}MHC-II^{+}) *(J)* derived from BM cells of *Nfatc1*$^{fl/fl}$ x *Cd11cCre* and *Nfatc1*$^{fl/fl}$ mice treated with HDM (n = 3/4). Representative dot plots are provided for each group. Data were analyzed by Mann-Whitney test or unpaired 2-tailed *t* test, and are presented as means ± SEMs. Schematics of *(A), (C)* and *(G)* were created by BioRender.com.

a 10-minute treatment with Mouse TruStain FcX Antibody (anti-mouse CD16/32, BioLegend, San Diego, Calif, catalog 101320) at RT to mitigate potential nonspecific antibody binding. Subsequently, the cells were stained with mouse antibodies targeting CD11c fluorescein isothiocyanate (FITC), sialic acid immunoglobulin-like lectin (Siglec)-F BV510, and CD45 AF700 (see Table E5 in the Online Repository available at www.jaci-global.org) for 20 minutes, following the protocol described below, and were then measured on the FACSCanto II benchtop analyzer (BD Biosciences, Heidelberg, Germany).

Organ isolation

After humanely killing the animal, lungs and spleen were aseptically removed. The thorax was disinfected and laterally opened on both sides to expose the lungs. A portion of lung tissue was placed into a specialized embedding cassette and fixed in a 4% formaldehyde solution for subsequent histologic analysis. Another piece of lung tissue was stored in a 1.5 mL Eppendorf tube at −80°C for future RNA analysis. The remaining lung tissue was transferred to 5 mL RPMI 1640 medium with 1% penicillin/streptomycin for

immediate isolation of lung cells. To remove the spleen, the left flank of the mouse was disinfected and the skin removed with scissors to expose the spleen. The entire spleen was then carefully excised and placed in 5 mL RPMI 1640 medium with 1% penicillin/streptomycin on ice until further processing.

Isolation and culture of total lung and splenic cells

Under sterile conditions and following a standardized protocol, total cells were isolated from lung and spleen tissues. Lung tissue was minced, then gently shaken in 10 mL of collagenase (Sigma-Aldrich)/DNase (Roche, Mannheim, Germany) solution for 45 minutes at 37°C. After enzymatic digestion, the cells were separated by homogenizing the tissue through a 40 μm cell strainer with a syringe plunger. The cell suspension was centrifuged (1500 rpm, 10 minutes, 4°C), and erythrocytes were lysed using 10 mL ACK lysis buffer, followed by another centrifugation (1500 rpm, 5 minutes, 4°C). The supernatant was discarded, and the cells were washed with 10 mL PBS. Slow pipetting and a horizontal pipette position helped remove remaining fat from the cell suspension. After another centrifugation (1500 rpm, 5 minutes, 4°C), the cells were resuspended in 10 mL PBS and counted using a Neubauer chamber and trypan blue. The same procedure was used for spleen cells, omitting the enzymatic digestion step. The tissue was immediately pushed through the cell strainer. All subsequent steps were identical to those for lung cells.

For lung cell or splenic cell culture with αCD3/28, the cell culture plate was precoated with 0.5 μg/mL αCD3 (BioLegend) in 0.1 mol sodium bicarbonate buffer (Carl Roth) for 1 hour at 37°C. After washing with PBS, cells were cultured in R10 medium (10% fetal bovine serum, 1% L-glutamine, 1% penicillin/streptomycin in RPMI 1640) with 1 μg/mL αCD28 (BioLegend) added. After 48 hours' cell culture at 37°C and 5% CO_2, supernatants and cells were collected. For the splenic CD4 cells cultured for 6 days, 5 ng/mL of IL-2 was supplemented every other day.

Splenic CD11c and CD4 cell sorting

For the sorting of splenic CD11c and CD4 cells, the procedure began by blocking nonspecific binding in total isolated splenic cells. Mouse TruStain FcX Antibody (anti-mouse CD16/32, BioLegend, catalog 101320) was used at a 1:100 dilution for 10 minutes at RT in the absence of light. After blocking, the cells were incubated for 25 minutes in a 500 μL MasterMix containing CD3 phycoerythrin (PE), CD4 BV421, and CD11c allophycocyanin–Cy7 (APC-Cy7) antibodies (Table E1) at RT. The staining process was halted with fluorescence-activated cell sorting (FACS) buffer, followed by centrifugation to remove the supernatant. Subsequently, the cells were resuspended in FACS buffer, which prepared them for sorting at the core unit for cell sorting at Friedrich-Alexander-University Erlangen-Nürnberg. The sorted cells were further used for RNA isolation and analysis. Alternatively, $CD4^+$ or $CD11c^+$ cells for cell culture were prepared by using magnetic cell sorting with mouse CD4 (L3T4) beads (Miltenyi Biotec, San Diego, Calif) and mouse CD11c MicroBeads UltraPure (Miltenyi Biotec), respectively. Initially, CD11c cells were isolated, followed by the isolation of CD4 cells from the CD11c-negative fraction. These isolation procedures strictly adhered to the manufacturer's instructions.

Bone marrow cell isolation and bone marrow–derived DC differentiation

The mice's hind legs were disinfected with 70% ethanol. The skin and muscle around the femur and tibia were removed to expose the bones, which were then excised, with all attached tissues cleared. These bones were again disinfected and rinsed with PBS before extracting bone marrow (BM). The bone ends were cut to access the marrow, which was flushed into a 50 mL centrifuge tube using a PBS-filled syringe. The marrow was then filtered through a 40 μm cell strainer into a new tube and centrifuged (1500 rpm, 5 minutes, 4°C) to form a single-cell suspension. Red blood cells in the sample were eliminated using ACK lysis buffer, followed by another centrifugation (1500 rpm, 5 minutes, 4°C). The resulting BM cells were resuspended in PBS, and their concentration was determined for use in cell culture or flow cytometry analysis.

To differentiate them into DCs, 2 million BM cells were suspended in 10 mL R10 medium and stimulated with 20 ng/mL recombinant granulocyte-macrophage colony-stimulating factor (rGM-CSF; ImmunoTools, Friesoythe, Germany) in a petri dish (Corning, Corning, NY, catalog 351029). They were incubated at 37°C and 5% CO_2. On day 3, 10 mL of R10 with rGM-CSF was added. On day 6, the top 10 mL was replaced with fresh R10/rGM-CSF medium. Culture continued until day 8, when cells were collected for flow cytometry analysis.

Flow cytometry analysis

For evaluation by flow cytometry, cells, either freshly isolated or cultured, were gathered and placed in flow cytometry tubes. This was followed by a rinse with PBS. The Zombie Aqua Fixable Viability Kit (BioLegend) was used to gauge cell viability, utilizing a 1:500 dilution in PBS. This staining was performed for 15 minutes at RT, shielded from light, in adherence to the manufacturer's guidelines. The staining was then neutralized with a FACS buffer composed of PBS, EDTA (Lonza, Basel, Switzerland), and 2% fetal calf serum. A centrifugation step at 1500 rpm for 5 minutes at 4°C followed.

To counteract potential nonspecific antibody binding, cells underwent a 10-minute treatment with anti-mouse or human TruStain FcX Antibody (anti-mouse CD16/32 [clone 93], BioLegend; anti-human CD16 [clone 3G8], αCD32 [clone FUN-2]/αCD64 [clone 10.1], BioLegend) at RT. After centrifugation and removal of the supernatant, the cells were resuspended into the antibody-laden MasterMix in FACS buffer. Each specimen was provided with 50 μL of the MasterMix in FACS buffer and underwent staining for 20 minutes at RT. This staining process was halted using FACS buffer, and another round of centrifugation ensued. This procedure targeted the staining of cell surface markers.

For analyzing intracellular proteins, such as transcription factors, the Foxp3/Transcription Factor Staining Buffer Set from Thermo Fisher Scientific was used. After surface staining, the cells were further fixed with 150 μL PermFix (diluted 1:4 in fixation diluent) for 35 minutes at 4°C in the dark. The PermFix was then removed by centrifugation (1500 rpm, 5 minutes, 4°C). The intracellular proteins were stained with 60 μL MasterMix consisting of PermWash (diluted 1:10 in double-distilled H_2O) and the desired antibodies, and incubated for 30 minutes at 4°C in the dark. The reaction was stopped by adding 200 μL of PermWash, followed by centrifugation (1500 rpm, 5 minutes,

4°C). Finally, the cells were resuspended in 200 μL of new FACS buffer for measurement using the FACSCanto II or Symphony A1 devices (BD Biosciences). The antibodies we used are listed in Tables E5 and E6 in the Online Repository available at www.jaci-global.org.

$CD4^+$ T-cell proliferation assay

The method for proliferation assay involved utilizing the CellTrace Violet kit to monitor cell proliferation through dye dilution in live cells. Specifically, isolated $CD4^+$ T cells were stained with CellTrace Violet staining solution (Thermo Fisher Scientific, catalog C34557) for 20 minutes in a 37°C water bath, with 1 million cells stained using 1 mL of the 5 μmol CellTrace Violet solution. After the staining process, R10 medium was introduced to the cells to absorb any excess unbound dye, and this mixture was incubated for an additional 5 minutes. Following this, the cells underwent centrifugation for 5 minutes at 1064 rpm, and the resulting cell pellet was carefully resuspended in prewarmed R10 medium. For the DC–T-cell coculture, a total of 180,000 stained $CD4^+$ T cells and 20,000 unstained $CD11c^+$ cells (DC:T = 1:9) were combined in a well of a 96-well U-bottom plate in the presence of 50 μg/mL HDM. After 4 days of cell culture, the cells were collected and subjected to analysis using a FACSCanto II device (BD Biosciences) equipped with a 405 nm excitation source and a 450/40 bandpass emission filter.

ELISA

The levels of total IgE in human serum were measured by electrochemiluminescence immunoassay on a cobas e 601 analyzer (Roche) according the manufacturer's instructions. Allergen-specific IgE in the AZCRA cohort was assessed using the radioallergosorbent test. Both assays were conducted at the Division of Pediatrics' research laboratory in Erlangen, Germany. Additionally, the levels of total IgE in mouse serum and IL-5 in cell culture supernatants were quantified using the OptEIA sandwich ELISA kits from BD Biosciences. The ELISA procedures were meticulously performed in accordance with the manufacturer's instructions.

Real-time quantitative PCR

After collection, cells were preserved in QIAzol Lysis Reagent (Qiagen, Hilden, Germany) for RNA extraction, in line with the guidelines provided by the manufacturer. This RNA was then transformed into cDNA utilizing the RevertAid First Strand cDNA Synthesis Kit (Thermo Fisher Scientific) following the prescribed protocol of the manufacturer. The real-time quantitative PCR (qPCR) analyses were performed using iTaq Universal SYBR Green Supermix (Bio-Rad, Hercules, Calif) and gene-specific primers sourced from Eurofins-MWG-Operon (Ebersberg, Germany). The primer sequences are listed in Table E4 in the Online Repository available at www.jaci-global.org. qPCR was executed using the CFX-96 Real-Time PCR Detection System (Bio-Rad). Data analysis was carried out by CFX Manager 3.0 software. The levels of transcripts were ascertained by the $2^{-\Delta\Delta Ct}$ method. Hypoxanthine phosphoribosyltransferase (aka HPRT) gene expression was used as an internal standard, and normalization was performed against the cycle threshold (C_t) values of the control samples.

Bulk RNA sequencing

To study the transcriptional landscape, total RNA was extracted from cells preserved in RNA stabilization solution (RLT buffer) and stored at −80°C. Quality control and sequencing were conducted by Novogene (Munich, Germany). RNA integrity was checked using an Agilent Bioanalyzer (Agilent Technologies, Santa Clara, Calif), excluding samples with an RNA integrity number below 7. Library preparation involved enriching mRNA using poly-T oligo–attached magnetic beads, followed by mRNA fragmentation and cDNA synthesis using random hexamer primers and dTTP for a nondirectional library. Library quality was assessed using Qubit, real-time PCR, and Bioanalyzer. Sequencing was performed on Illumina (San Diego, Calif) platforms. Raw sequencing data underwent quality control using FastQC, including adapter and low-quality base trimming with Trimmomatic. Reads were aligned to the mouse reference genome (*Mus musculus,* GRCm39/mm39). Gene expression quantification was done using featureCounts, with differential analysis performed by R software (R Project; www.r-project.org) using DESeq2.

Statistical analysis

In this study, cell percentages were accurately determined by FlowJo 10.9 (Becton Dickinson, Franklin Lakes, NJ) or Kaluza Analysis Software (Beckman Coulter, Fullerton, Calif), with further statistical analysis performed by GraphPad Prism 9 software (GraphPad Software, La Jolla, Calif), presenting results as means ± SEMs. For 2-group comparisons, the unpaired Student 2-tailed *t* test or the Mann-Whitney test for normally and nonnormally distributed data, respectively, were applied. One-way ANOVA was used for analyzing multiple groups based on a single independent variable, while 2-way ANOVA was used for data involving 2 independent variables, including their interaction effects. Additionally, correlations were discerned through simple linear regression. $P < .05$ signifies statistical significance. RNA sequencing data were analyzed by DESeq2 for the identification of differentially expressed genes, with gene enrichment analysis and visualization conducted in R software, ensuring a comprehensive and robust statistical evaluation.

RESULTS

Nfatc1 in $CD4^+$ T-cell–mediated asthma in HDM mouse model

To gain insights relevant to human asthma, we used HDM, a clinically significant allergen, to induce asthma in mice, and compared *Nfatc1*$^{fl/fl}$ and *Nfatc1*$^{fl/fl}$ x *Cd4Cre* mice, where the latter lacks *Nfatc1* in $CD4^+$ T cells (Fig 1, *A*). A significant reduction in the percentage of $CD4^+$ T cells was observed in the spleens of *Nfatc1*$^{fl/fl}$ x *Cd4Cre* mice, while $CD4^+$ T-cell levels in the lungs remained comparable to those in control mice (see Fig E1, *A* and *B,* in the Online Repository available at www.jaci-global.org). By analyzing splenic $CD4^+$ $CD3^+$ T-cell transcriptomes via RNA sequencing (RNA-Seq), distinct expression patterns emerged between the groups, underscoring *Nfatc1*'s key role in $CD4^+$ T cells

in asthma pathology, as shown in the principal component analysis (PCA) results (Fig 1, *B* and *C*).

Transcriptome analysis revealed that *Nfatc1* deficiency in $CD4^+$ T cells significantly diminishes T-cell activation and T_H2 polarization gene expression. The reduced expression of *Jun* and *Fos* suggests impaired T-cell activation (Fig 1, *D*). Moreover, the expression levels of the T_H2 cytokines *Il5, Il10,* and *Il13;* peroxisome proliferator–activated receptor γ (*Pparg*); and amphiregulin (*Areg*) in *Nfatc1*-deficient $CD4^+$ T cells were decreased (Fig 1, *D,* and Fig E1, *C* and *D*), suggesting an inhibited T_H2 effector function without *Nfatc1* in $CD4^+$ T cells. This was further supported by a decrease in $Gata3^+$ T_H2 cells in the lungs of $Nfatc1^{fl/fl}$ x *Cd4Cre* asthmatic mice (Fig 1, *E*), accompanied by a reduction in *Il13* expression (Fig 1, *F*).

Consistent with a diminished T_H2 response, we found a decrease in the percentage of inflammatory eosinophils (iEOS) in the $Nfatc1^{fl/fl}$ x *Cd4Cre* asthmatic mice (Fig 1, *G,* and Fig E1, *E*). Moreover, $Nfatc1^{fl/fl}$ x *Cd4Cre* mice treated with HDM showed a significant increase in the total regulatory T-cell population in the lungs compared to controls (Fig 1, *H*), indicating an enhanced immunosuppressive response in these mice.

To evaluate allergic responses, we measured total serum IgE levels in both mouse genotypes after exposure to HDM. Remarkably, the mice with *Nfatc1* deletion in T cells exhibited significantly lower serum IgE levels than the $Nfatc1^{fl/fl}$ control mice (Fig 1, *I*), aligning with fewer lung mast cells (Fig 1, *J,* and Fig E1, *F*). These findings suggest that *Nfatc1*'s absence in T cells leads to a marked reduction in allergic symptoms in the HDM-induced asthma model, highlighting the significant role of *Nfatc1* in T cells in mediating allergic reactions.

Impaired differentiation of splenic and BM-DCs due to *Nfatc1* deficiency in CD11c cells

Considering DCs' crucial role in T-cell responses in asthma and their NFATc1 expression, we expanded our study to investigate the role of NFATc1 in DCs using $Nfatc1^{fl/fl}$ x *Cd11cCre* conditional knockout mice, where *Nfatc1* is deleted in $CD11c^+$ cells (Fig 2, *A*).

In our study, RNA-Seq of splenic $CD11c^+$ cells from $Nfatc1^{fl/fl}$ and $Nfatc1^{fl/fl}$ x *Cd11cCre* mice in the HDM-induced asthma model revealed distinct transcriptomic profiles (Fig 2, *B-F*). The separation observed in the PCA analysis (Fig 2, *D*), combined with the number of unique differentially expressed genes identified between $CD11c^+$ cells from control and $Nfatc1^{fl/fl}$ x *Cd11cCre* mice (Fig 2, *E*), highlights the distinct gene expression patterns between these 2 groups. *Nfatc1* deficiency led to the downregulation of key genes involved in DC activation and function, including major histocompatibility complex (MHC) class II molecules (*H2-M2, H2-M5, H2-Eb2*), the chemokine receptor *Ccr7,* and costimulatory molecules (*Cd80, Cd86, Cd40*). This downregulation suggests impaired antigen presentation, reduced DC migration, and a decreased ability to prime T cells effectively (Fig 2, *F*). Furthermore, *Nfatc1*-deficient DCs showed reduced expression of pattern recognition receptors (eg, *Clec4, Tlr3, Trl11*), suggesting a diminished pathogen recognition capacity. The *Nfatc1* deletion also seemed to affect various DC subsets, indicated by decreased expression of markers such as *Zbtb46* (a marker for conventional DCs), *Cd8a, Xcr1,* and *Cadm1* (markers for conventional DC1), *Sirpa* (a classic marker for conventional DC2), and *Cd209a* (a marker for monocyte-derived DCs or plasmacytoid DCs). Additionally, there was a lower expression of inflammatory genes (eg, *Tnfrsf4, Il1b*), possibly altering inflammatory responses in asthma (Fig 2, *F*).

To further elucidate *Nfatc1*'s impact on DC differentiation, we conducted a BM-derived DC differentiation assay using BM cells from both $Nfatc1^{fl/fl}$ and $Nfatc1^{fl/fl}$ x *Cd11cCre* mice (Fig 2, *G*). Our analysis identified 2 distinct DC populations, one with high MHC-II expression ($MHC\text{-}II^{hi}$ DCs) and the other with low MHC-II expression ($MHC\text{-}II^{dim}$ DCs) (Fig 2, *H* and *I*). Although the reductions observed in these individual subsets did not reach statistical significance, the overall DC population derived from $Nfatc1^{fl/fl}$ x *Cd11cCre* mice treated with HDM exhibited a statistically significant decrease (Fig 2, *H-J*). These findings highlight *Nfatc1*'s critical role in guiding the differentiation of DCs, particularly in the context of asthma pathophysiology.

Alterations in lung DC composition due to *Nfatc1* deficiency in CD11c cells in experimental asthma

In asthma pathogenesis, DCs originate from BM precursors or monocytes. Impaired DC differentiation from BM cells of $Nfatc1^{fl/fl}$ x *Cd11cCre* mice in response to HDM exposure led us to hypothesize that *Nfatc1* expression in $CD11c^+$ cells is crucial for proper differentiation and maturation of lung DCs, thus influencing the immune response in asthma.

To validate this hypothesis, we used flow cytometry to analyze the lung DC populations in the mice after HDM treatment. As we thought, a significant reduction in the DC population was found in $Nfatc1^{fl/fl}$ x *Cd11cCre* asthmatic mice compared to control mice (Fig 3, *A* and *B*). This reduction was particularly notable in the $MHC\text{-}II^{hi}$ DC subset, indicative of mature DCs, but not in the $MHC\text{-}II^{dim}$ subset (Fig 3, *C* and *D*). No significant differences in the lung DCs were detected at baseline (see Fig E3, *A,* in the Online Repository available at www.jaci-global.org). These results suggest that *Nfatc1* in CD11c cells plays a crucial role in DC maturation in the context of asthma.

Further analysis of lung $CD11b^+$ DCs in the HDM-induced asthma model, which are known to drive T_H2 responses in asthma,[21] revealed significant reductions in both high- and low-expression $CD11b^+$ DC groups in *Nfatc1*-deficient mice (Fig 3, *E* and *F*), with no change in $CD11b^-$ DCs (Fig E3, *B*). Additionally, DCs from *Nfatc1*-deficient mice displayed lower high-affinity IgE receptor (FcεRI) expression (Fig 3, *G*), implicating *Nfatc1* in IgE receptor regulation. We also noted reduced C-C chemokine receptor type 7 (CCR7) expression, which is essential for DC migration and function,[22,23] in both $MHC\text{-}II^{dim}$ and $MHC\text{-}II^{hi}$ DC subsets in *Nfatc1*-deficient mice (Fig 3, *H* and *I*), aligning with RNA-Seq findings of decreased *Ccr7* transcription in *Nfatc1*-deficient splenic $CD11c^+$ cells (Fig 2, *F*).

Collectively, the notable changes observed in the lung DCs due to *Nfatc1* deficiency in the HDM-induced asthma model point to an immature state of these cells, which compromises their ability to effectively promote T-cell activation.

Attenuation of T-cell responses, especially T_H2 responses, in lungs of HDM-induced asthmatic mice with *Nfatc1* deficiency in $CD11c^+$ cells

Because we observed alterations in DCs due to *Nfatc1* deficiency in CD11c cells, we evaluated the T-cell response in $Nfatc1^{fl/fl}$ x *Cd11cCre* mice. Initially, we analyzed total $CD4^+$

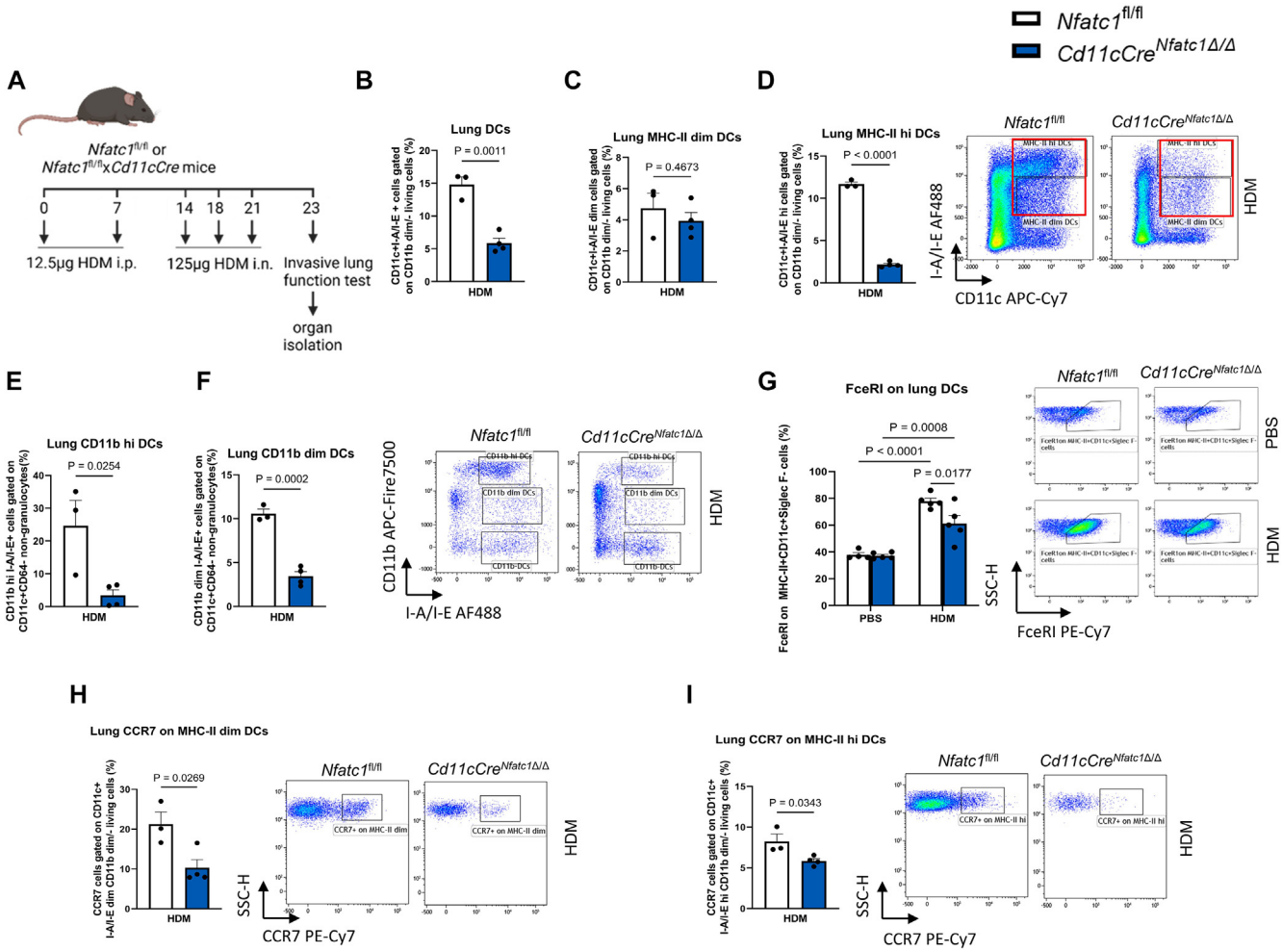

FIG 3. Effects of *Nfatc1* deficiency in CD11c cells on lung DCs. **A,** HDM-induced asthma model in *Nfatc1*$^{fl/fl}$ and *Nfatc1*$^{fl/fl}$ x *Cd11cCre* mice. **B-D,** Flow cytometry analysis depicting proportions of CD11c^{+}MHC-II^{+} total DCs, CD11c^{+}MHC-II^{dim} DCs, and CD11c^{+}MHC-II^{hi} DCs in lungs of *Nfatc1*$^{fl/fl}$ x *Cd11cCre* and *Nfatc1*$^{fl/fl}$ mice treated with HDM (n = 3/4). **E** and **F,** Flow cytometric quantification of DC populations with high and low CD11b expression in lungs of both genotypes of mice treated with HDM (n = 3/4). **G,** Flow cytometry analysis of FcεRI expression on DCs (CD11c^{+}MHC-II^{+}Siglec-F^{+}) in lungs of both genotypes of mice treated with HDM (n = 4/5/5/5). **H** and **I,** Flow cytometry analysis of CCR7 expression on MHC-II^{dim} DC populations and MHC-II^{hi} DC populations in lungs of both genotypes of HDM-treated mice (n = 3/4). Representative dot plots are shown for each group. Data were analyzed by unpaired 2-tailed *t* test, Mann-Whitney test, or ordinary 2-way ANOVA, and are presented as means ± SEMs.

T-cell population within the pulmonary tissue of mice. Under basal conditions, the CD4^{+} T-cell prevalence in the lungs of *Nfatc1*$^{fl/fl}$ x *Cd11cCre* mice was similar to that seen in *Nfatc1*$^{fl/fl}$ mice (Fig 4, *A*). However, under asthmatic conditions induced by HDM, *Nfatc1*$^{fl/fl}$ x *Cd11cCre* mice showed a significant decrease in the lung CD4^{+} T cells compared to *Nfatc1*$^{fl/fl}$ mice (Fig 4, *A*). Furthermore, lung cell cultures derived from these mice also exhibited a notable decrease in CD4^{+} T-cell populations on re-exposure to HDM antigens *in vitro* (Fig 4, *B* and *C*). This reduction aligns with the diminishment in DC population and the downregulation of CD40 expression on these DCs (Fig 4, *D* and *E*).

To further confirm the impact of *Nfatc1* in CD11c cells on CD4 T-cell proliferation, we conducted a cell proliferation assay via DC–T-cell coculture, where the CD4^{+} T cells were labeled with CellTracer (Fig 4, *F*). Results showed reduced CD4^{+} T-cell proliferation when cocultured with CD11c cells lacking *Nfatc1,* relative to cocultures with CD11c cells retaining *Nfatc1* expression (Fig 4, *G*). This indicates that *Nfatc1* deficiency in CD11c cells results in reduced capacity for T-cell activation. Additionally, a decrease in IL-5 production was noted in the splenic CD4 cell cultures from the *Nfatc1*$^{fl/fl}$ x *Cd11cCre* mice, implying a diminished T_H2 polarization (Fig 4, *H*). Indeed, a significant reduction in the T_H2 cell population and a lower *Il13* expression were observed in the lungs of knockout mice treated with HDM (Fig 4, *I* and *J*), further emphasizing the critical role of *Nfatc1* in CD11c cells in regulating the T_H2 response in allergic asthma.

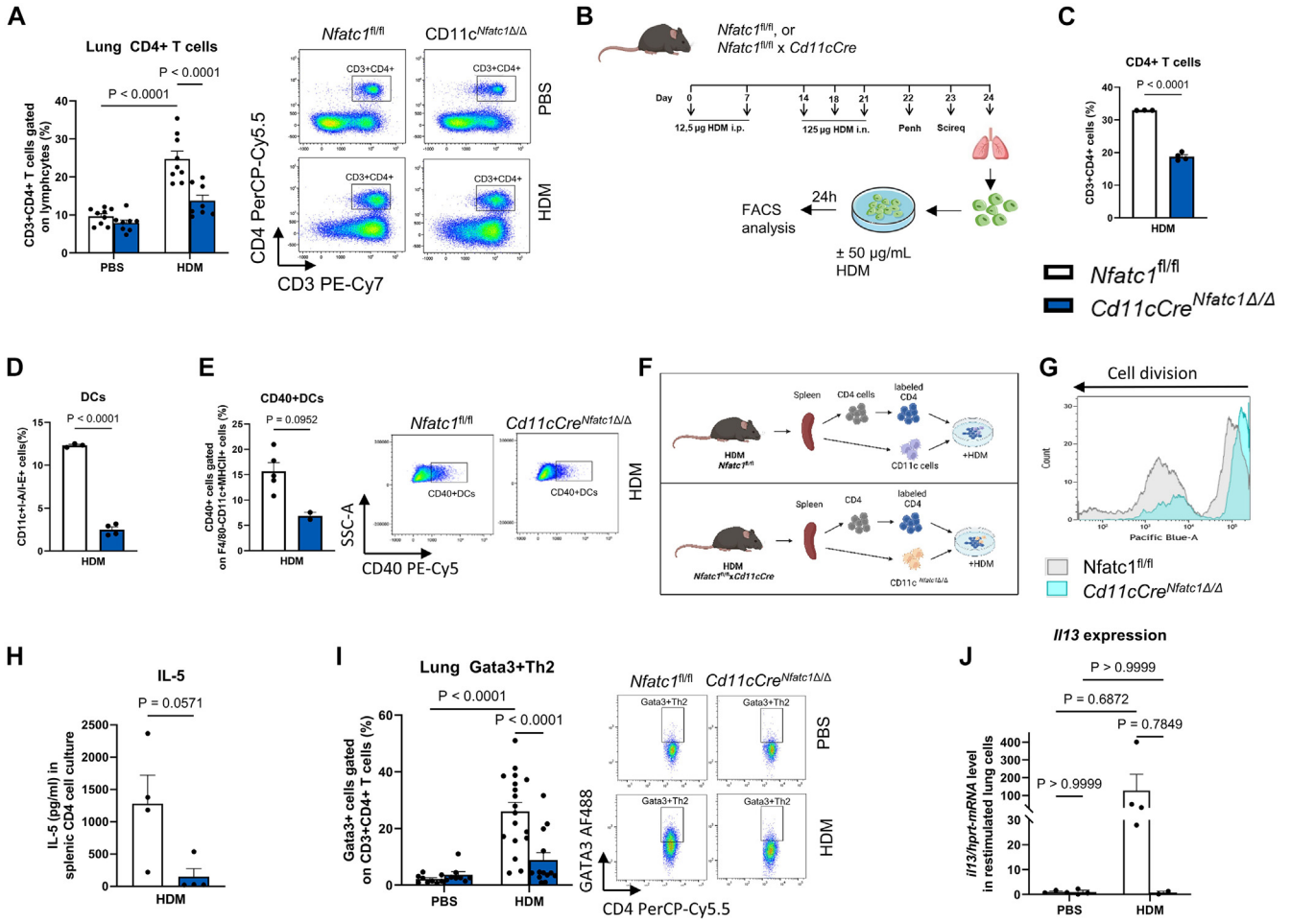

FIG 4. *Nfatc1* deficiency in CD11c cells diminished T-cell proliferation and T_H2 response in asthma model induced by HDM. **A,** Flow cytometry analysis of lung $CD3^+CD4^+$ cells (%) in *Nfatc1*$^{fl/fl}$ x *Cd11cCre* mice and *Nfatc1*$^{fl/fl}$ mice treated with or without HDM (n = 9/8/9/8). **B,** Experimental design of lung cell culture study. **C-E,** Flow cytometry analysis of $CD4^+$ T cells, DCs, and $CD40^+$ DCs in lung cell cultures from *Nfatc1*$^{fl/fl}$ x *Cd11cCre* and *Nfatc1*$^{fl/fl}$ asthmatic mice in presence of 50 µg/mL HDM (n = 2-4). **F,** Schematic showing coculture of DCs and T cells with HDM. $CD4^+$ cells are labeled with CellTracer for tracking cell growth by flow cytometry. **G,** Flow cytometry analysis depicting proliferation of $CD4^+$ T cells. **H,** ELISA quantification of IL-5 from 6-day cultured splenic $CD4^+$ T cells restimulated with anti-CD3/28 and in presence of IL-2 (n = 4/4). **I,** Flow cytometry analysis of lung $Gata3^+$ T_H2 cells (%) in *Nfatc1*$^{fl/fl}$ x *Cd11cCre* mice and *Nfatc1*$^{fl/fl}$ mice treated with HDM (n = 9/8/18/13); representative dot plot is shown for each group. **J,** *Il13 mRNA* level relative to *Hprt* in anti-CD3/28 restimulated total lung cells was quantified by qPCR (n = 3/3/4/2). Data were analyzed by unpaired 2-tailed *t* test, Mann-Whitney test, or ordinary 2-way ANOVA, and are presented as means ± SEMs. Schematics of *(B)* and *(F)* were created by BioRender.com. *Hprt,* Hypoxanthine phosphoribosyltransferase.

Reduced allergic traits and lung eosinophilic inflammation in asthmatic mice with *Nfatc1*-depleted CD11c cells

In our study, we assessed airway hyperresponsiveness of the mice by measuring respiratory resistance in response to incremental doses of methacholine (Fig 5, *A*). Notably, mice with *Nfatc1* deficiency in CD11c cells exhibited a trend toward reduced airway hyperresponsiveness, as evidenced by lower respiratory system resistance values compared to the control group (Fig 5, *B*). When the methacholine doses were increased up to 100 mg/mL, both genotypes of HDM-treated mice showed a slight decrease in airway hyperresponsiveness (Fig 5, *B*).

We also measured serum IgE levels, an allergy marker in asthma, and found significantly higher levels in control mice upon HDM challenge (Fig 5, *C*), whereas the conditional *Nfatc1*$^{fl/fl}$ x *Cd11cCre* knockout mice did not show a similar increase in IgE levels after HDM treatment (Fig 5, *C*). This observation prompted an investigation into mast cells, which are crucial in IgE-driven allergic asthma. We assessed the presence of FcεRI-expressing mast cells in the lungs of both genotypes of mice. Consistent with the lower IgE production, PBS-treated mice exhibited a low percentage of lung mast cells. Notably, in the HDM-treated group, the knockout mice had a significantly reduced percentage of mast cells in their lungs compared to controls (Fig 5, *D*). These

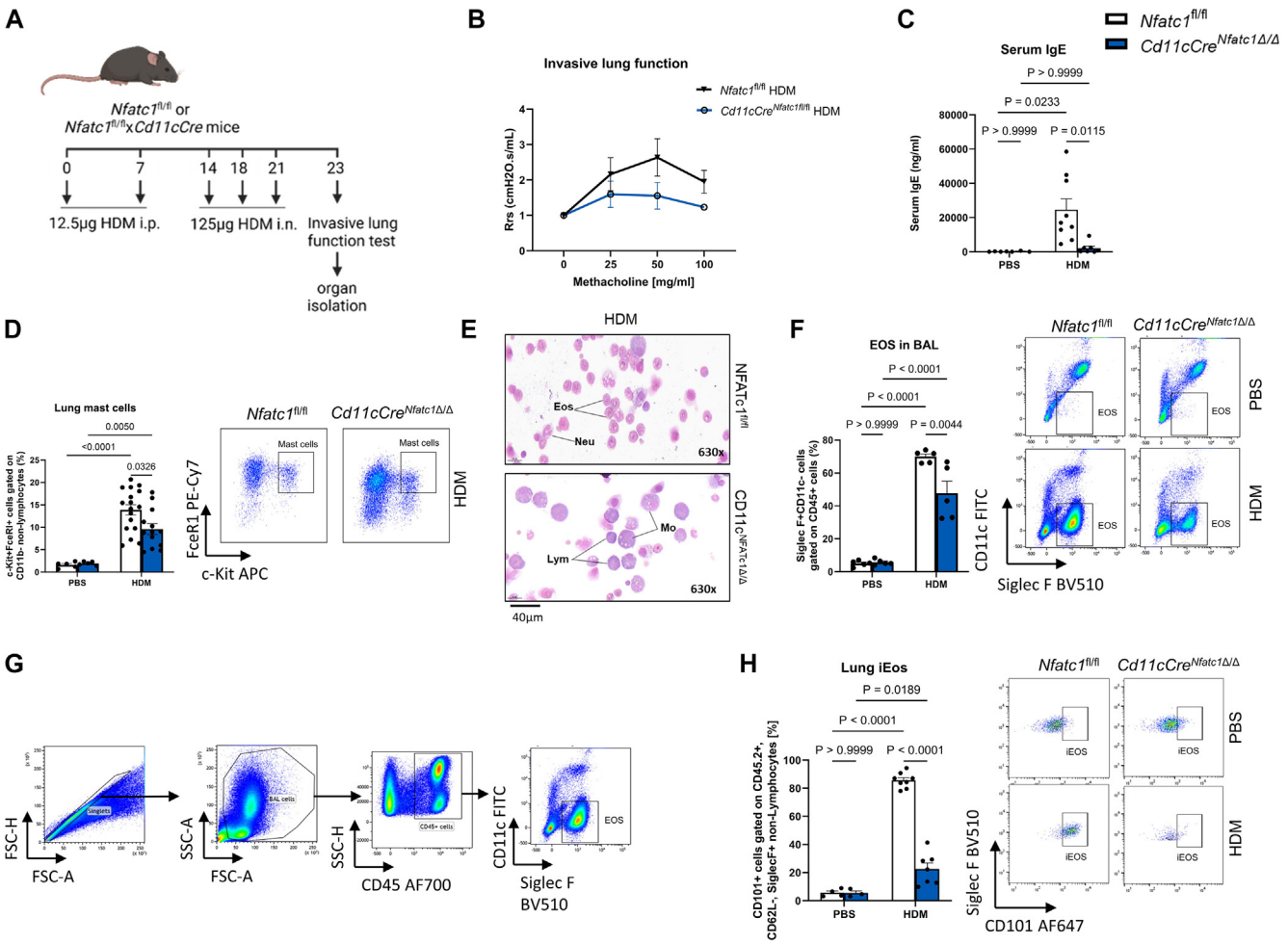

FIG 5. Decreased IgE-mediated allergy and lung eosinophil inflammation in asthmatic mice with CD11c-specific *Nfatc1* depletion. **A,** HDM-induced asthma model in *Nfatc1*$^{fl/fl}$ and *Nfatc1*$^{fl/fl}$ x *Cd11cCre* mice. **B,** Invasive plethysmography results on day 23, comparing airway responsiveness to increasing methacholine doses in both mouse types (n = 3-9). **C,** Serum IgE measured by ELISA (n = 4/3/9/7). **D,** Flow cytometry analysis showing percentage of mast cells (CD117/c-kit^{+}FcεRI^{+}CD11b^{-}) in lung of *Nfatc1*$^{fl/fl}$ x *Cd11cCre* mice and *Nfatc1*$^{fl/fl}$ mice treated with or without HDM (n = 5/5/12/8). **E,** Cytologic analysis of BAL cells from HDM-treated *Nfatc1*$^{fl/fl}$ and *Nfatc1*$^{fl/fl}$ x *Cd11cCre* mice. **F** and **G,** Flow cytometry analysis of percentage of eosinophils (Siglec-F^{+}CD11c^{-}CD45^{+}) in BAL, comparing *Nfatc1*$^{fl/fl}$ x *Cd11cCre* and *Nfatc1*$^{fl/fl}$ mice, with or without HDM treatment, with representative dot plots (n = 5). **H,** Flow cytometry analysis of percentage of iEOS (CD45.2^{+}Siglec-F^{+}CD62L^{-}CD101^{+}) in lung, with representative dot plots (n = 4/3/8/7). Data were analyzed by ordinary 2-way ANOVA, and are presented as means ± SEMs.

results suggest that *Nfatc1* in CD11c cells significantly enhances allergic responses in asthma.

In the HDM-induced asthma model, upon examination of BAL samples using cytospin techniques, a reduced number of eosinophils was observed in *Nfatc1*$^{fl/fl}$ x *Cd11cCre* mice compared to *Nfatc1*$^{fl/fl}$ controls (Fig 5, *E*). This finding was consistent with the eosinophil percentages obtained from the flow cytometry analyses (Fig 5, *F* and *G*). Furthermore, both genotypes of mice exposed to HDM exhibited a significant increase of iEOS in lung tissue compared to untreated mice (Fig 5, *H*). However, the *Nfatc1*$^{fl/fl}$ x *Cd11cCre* mice showed a notable reduction in the iEOS population compared to the *Nfatc1*$^{fl/fl}$ mice receiving HDM treatment (Fig 5, *H*), suggesting a potential attenuation of eosinophil-mediated inflammatory responses in asthma due to the targeted deletion of *Nfatc1* in CD11c-expressing cells.

Correlation between NFATc1^{+}CD4^{+} T-cell population in PBMCs and blood eosinophils in asthmatic patients

To elucidate the translational relevance of findings derived from murine models of asthma, we established the AZCRA cohort, including healthy controls and patients diagnosed with asthma (Fig 6, *A*, Table E1, Table E2). Within the AZCRA cohort, asthma patients and control subjects were divided into allergic and nonallergic subgroups using a 100 kU/L serum IgE threshold. Patients with allergic asthma showed

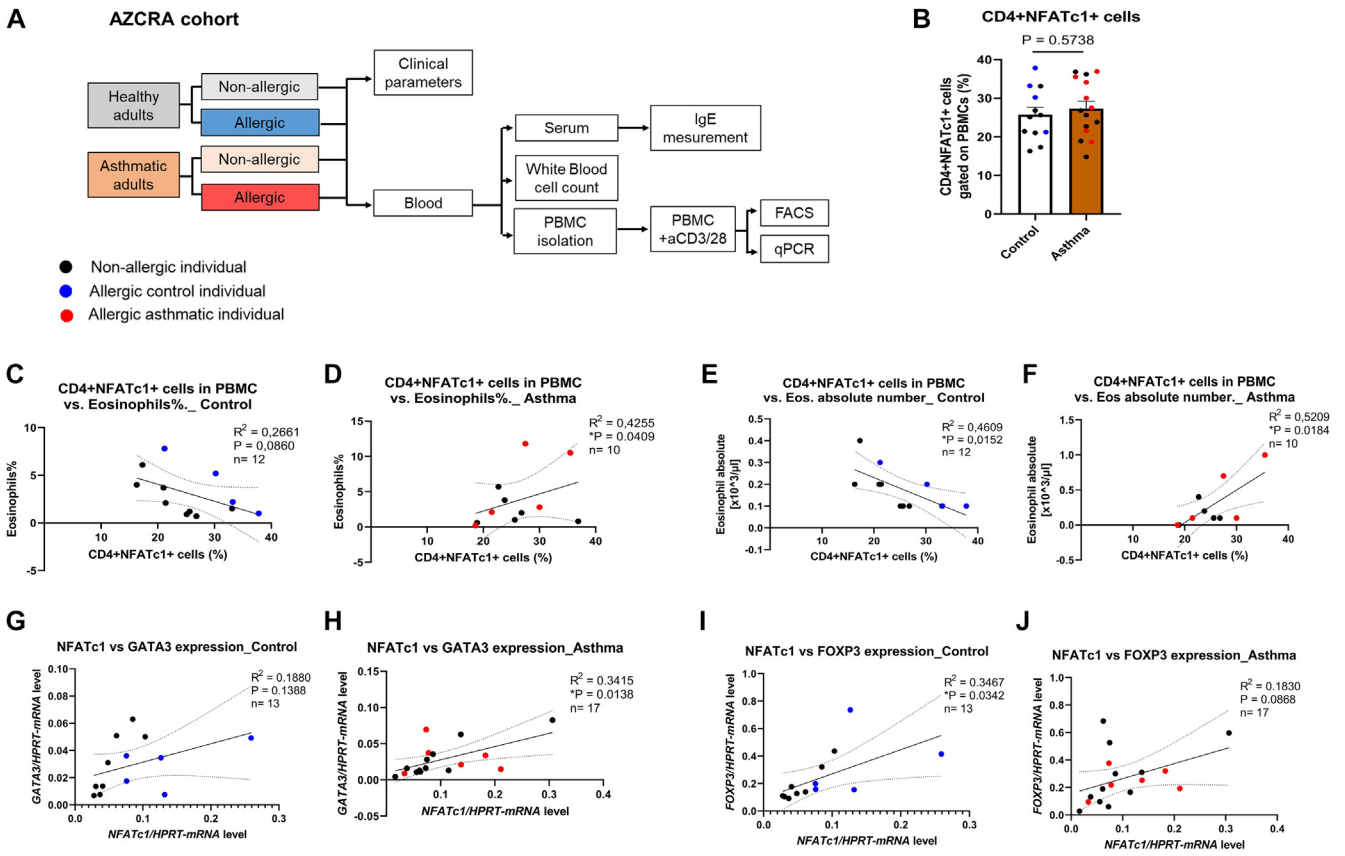

FIG 6. Analysis of CD4+NFATc1$^+$ cells within PBMCs from AZCRA cohort and its correlation with blood eosinophil levels. **A,** Experimental design showing methodology for AZCRA cohort study. **B,** Flow cytometry analysis comparing percentage of CD4$^+$NFATc1$^+$ T cells in anti-CD3/28 restimulated PBMCs between control subjects (n = 12) and asthmatic patients (n = 15) in AZCRA cohort. **C** and **D,** Correlation between CD4$^+$NFATc1$^+$ cell population and eosinophil percentage in controls (n = 12) and asthma patients (n = 10). **E** and **F,** Correlation between CD4$^+$NFATc1$^+$ cell population and eosinophil count in these groups. **G** and **H,** Correlations between relative NFATc1 mRNA level and GATA3 mRNA level in anti-CD3/28 restimulated PBMCs from controls (n = 13) and asthma patients (n = 17), respectively. **I** and **J,** Correlations between relative *NFATc1 mRNA* level and *FOXP3 mRNA* level in anti-CD3/28 restimulated PBMCs from controls (n = 13) and asthma patients (n = 17), respectively. *Black dots* indicate individuals without allergies (IgE <100 kU/L); *blue dots,* control individuals with allergies (IgE ≥100 kU/L); and *red dots,* asthmatic individuals with allergies (IgE ≥100 kU/L). Data were analyzed by unpaired 2-tailed *t* test for comparison and are presented as means ± SEMs. Correlations were determined by simple linear regression.

significantly elevated IgE levels versus allergic controls (see Fig E2, *A,* in the Online Repository available at www.jaci-global.org). We also performed allergen-specific IgE testing to detect sensitivities to a broad range of environmental allergens. Our analysis identified IgE specific to birch pollen, HDM (*D pteronyssinus*), and timothy grass pollen as the top 3 specific IgE detected in asthmatic patients (Fig E2, *B*). The detection of different allergen-specific IgE types in blood indicates the presence of various allergies. In the AZCRA cohort, 80% of asthma patients had at least one type of allergy, with many exhibiting sensitivities to multiple allergens (Fig E2, *C*). In contrast, only 35% of the control group showed any allergic response, and these allergic controls typically had fewer types of allergies (Fig E2, *D*). Additionally, asthma patients exhibited higher levels of C-reactive protein compared to controls (Fig E2, *E*), as well as a notable correlation between IgE levels and eosinophils, absent in controls, thus reinforcing the link between allergic inflammation and asthma pathophysiology (Fig E2, *F* and *G*). These characteristics of the AZCRA cohort provide a valuable human model for translating our findings from the HDM-induced asthma mouse model.

In the analysis of the AZCRA cohort, we compared the CD4$^+$NFATc1$^+$ cell populations in PBMCs restimulated with anti-CD3/CD28 for 4 days from both asthmatic patients and healthy controls (Fig 6, *A*). Our findings showed no statistically significant differences in the proportion of CD4$^+$NFATc1$^+$ cells between the asthma and control groups (Fig 6, *B*). However, in the correlation analysis, we observed an inverse correlation between the CD4$^+$NFATc1$^+$ cells and blood eosinophils in healthy control subjects (Fig 6, *C* and *E*), whereas this correlation was positive among asthmatic patients (Fig 6, *D* and *F*). Such differing patterns of correlation indicate a distinct immunologic context for the CD4$^+$NFATc1$^+$ T-cell population in healthy versus asthmatic individuals.

We further analyzed the restimulated PBMCs from asthmatic patients and healthy controls. Here, we found a significant correlation between *NFATc1* and *GATA3* expression, a relationship not seen in the control group (Fig 6, *G* and *H*). In contrast, in the control group, there was a significant correlation between *NFATc1* and *FOXP3* expression, which was absent in the asthma group (Fig 6, *I* and *J*). These observations suggest that in asthma patients, the $CD4^+NFATc1^+$ cell population is likely representative of T_H2 cells, which contribute to eosinophilic inflammation in allergic asthma. Conversely, in the control group, these $CD4^+NFATc1^+$ cells may be involved in immune suppression, as indicated by the corresponding increase in FOXP3 (forkhead box P3) expression, suggesting a potential regulatory function.

Elevated $CD11c^+NFATc1^+$ cells in PBMCs and their correlation with eosinophils in asthmatic patients

In our human study, we sought to translate and validate findings from a murine model featuring *Nfatc1* deficiency in $CD11c^+$ cells within the context of HDM-induced asthma. We focused on analyzing the $CD11c^+$ cell populations, specifically the $CD11c^+NFATc1^+$ subset, in freshly isolated PBMCs from individuals with and without asthma in the AZCRA cohort using flow cytometry. The results showed no significant differences in the overall $CD11c^+$ cell population between the control and asthma groups (Fig 7, *A* and *B*). However, we observed a significant increase in the $CD11c^+NFATc1^+$ subset in asthmatic patients compared to healthy subjects (Fig 7, *C*), indicating a potentially altered functional state of these cells in asthma, which may contribute to exaggerated immune responses.

Further investigations within the AZCRA cohort explored the correlation between $CD11c^+NFATc1^+$ cell population and circulating eosinophil level. Our findings revealed a positive correlation in both control and asthmatic subjects (Fig 7, *D* and *E*). Notably, this correlation reached statistical significance in the asthma group, but not in the control group (Fig 7, *D* and *E*). This outcome suggests a potential pathophysiologic significance of $CD11c^+NFATc1^+$ cells in asthma, particularly in their role in modulating eosinophilic responses. The presence of a significant correlation specifically in asthmatic patients, but not in healthy controls, points to a more critical or distinctive functional role for the $CD11c^+NFATc1^+$ cell population in the inflammatory response associated with asthma.

DISCUSSION

In this study, we explored the role of NFATc1 in T cells and $CD11c^+$ DCs in allergic asthma, utilizing an HDM-induced asthma model and analyzing data from the human AZCRA cohort. We confirmed and extended our previous studies that NFATc1 plays a crucial role in driving T_H2-mediated eosinophilic inflammation in both experimental and human asthma. Specifically, *Nfatc1* facilitates T_H2 polarization and effector function in $CD4^+$ T cells and is essential for DC differentiation and function in $CD11c^+$ cells, promoting T-cell activation and T_H2 polarization. Therefore, *Nfatc1* deficiency in both of these cell types leads to reduced T_H2 cells, eosinophils, and serum IgE levels in the context of asthma, thereby enhancing our understanding of the disease's underlying mechanisms and positioning NFATc1 as a promising target for therapeutic strategies.

Our findings demonstrate a significant reduction in splenic $CD4^+$ T cells in *Nfatc1*-deficient *Cd4Cre* mice treated with HDM, likely due to impaired survival or proliferation in the absence of *Nfatc1*. The literature highlights NFATc1's pivotal role in T-cell activation and proliferation, interacting with activator protein 1 complex, composed of Fos and Jun proteins.[8,9,24,25] Consistent with this, our research revealed that *Nfatc1* deficiency reduces the expression of *Fos* and *Jun* in $CD4^+$ T cells, which are crucial for T-cell activation. However, the observed reduction in splenic $CD4^+$ T cells might also result from increased migration to the lungs after HDM exposure. Because lung $CD4^+$ T-cell levels remain unchanged and because tracking markers were not used in this study, NFATc1's impact on T-cell recruitment to the lungs remains uncertain. Future studies with tracking markers are needed to clarify NFATc1's role in $CD4^+$ T-cell migration.

GATA3 (GATA-binding protein 3) is a crucial transcription factor for T_H2 identity and expression of the T_H2 cytokines *Il5, Il13,* and *Il10*.[26-28] NFATc1 can regulate T_H2 polarization and function and can work with GATA3 to enhance IL-5 production via interaction at the IL-5 gene locus.[29-31] In an ovalbumin-induced asthma model, *Nfatc1* deletion resulted in decreased type 2 cytokine production, while *Gata3* mRNA levels in the lung $CD4^+$ T cells remained unchanged.[14] However, in this HDM-induced asthma model, the mice with *Nfatc1* deletion in T cells showed reduced $Gata3^+$ T_H2 cells in the lung, along with lower *Il13* mRNA levels; decreased *Il5, Il10,* and *Il13* expression was also found in splenic $CD4^+$ T cells in the absence of *Nfatc1*. These findings suggest *Nfatc1*'s necessity for both Gata3 expression during T_H2 differentiation and the maintenance of effector functions in differentiated T_H2 cells in HDM-induced asthma. Pparg boosts T_H2 functions and lung inflammation in HDM-induced asthma,[32] while Areg, induced by IL-33 in memory T_H2 cells, promotes airway fibrosis through eosinophils.[33] The reduction of *Pparg* and *Areg* expression in $CD4^+$ splenic cells in the absence of *Nfatc1* also suggests suppressed T_H2 functions. Alongside the reduction in T_H2 cells, there was an increase in Treg cells in the lungs of *Nfatc1*-deficient *Cd4Cre* mice in the HDM-induced asthma model, indicating that alternative polarization pathways may become more prominent without *Nfatc1*.

Reduced lung iEOS, which drives asthma-related inflammation dependent on type 2 cytokine IL-5,[34,35] was found in the lung of mice with *Nfatc1* deficiency in $CD4^+$ T cells in the HDM-induced asthma model. This finding was translated in asthmatic patients, where significant correlations were found between $CD4^+NFATc1^+$ cells and blood eosinophils, as well as between *NFATc1* and *GATA3* expression, which were not found in the control group. These results emphasize the pivotal role of NFATc1 in CD4 cells in T_H2 responses and eosinophilic inflammation in the context of asthma. Compared to a previous study that reported that NFAT in $CD4^+$ T cells is required for eosinophils involved allergic airway inflammation,[36] our research further specifies that this effect is attributable to a specific member of the NFAT family, namely NFATc1.

In contrast, in healthy individuals, $CD4^+NFATc1^+$ T cells inversely correlated with eosinophils, while NFATc1 positively correlated with FOXP3 expression in restimulated PBMCs. This underscores NFATc1's regulatory role in FOXP3 expression, hinting at a potential link between $CD4^+NFATc1^+$ T cells and Treg cells. In the mouse models of asthma, we found that the deletion of *Nfatc1* in $CD4^+$ T cells induced Treg cells, indicating a

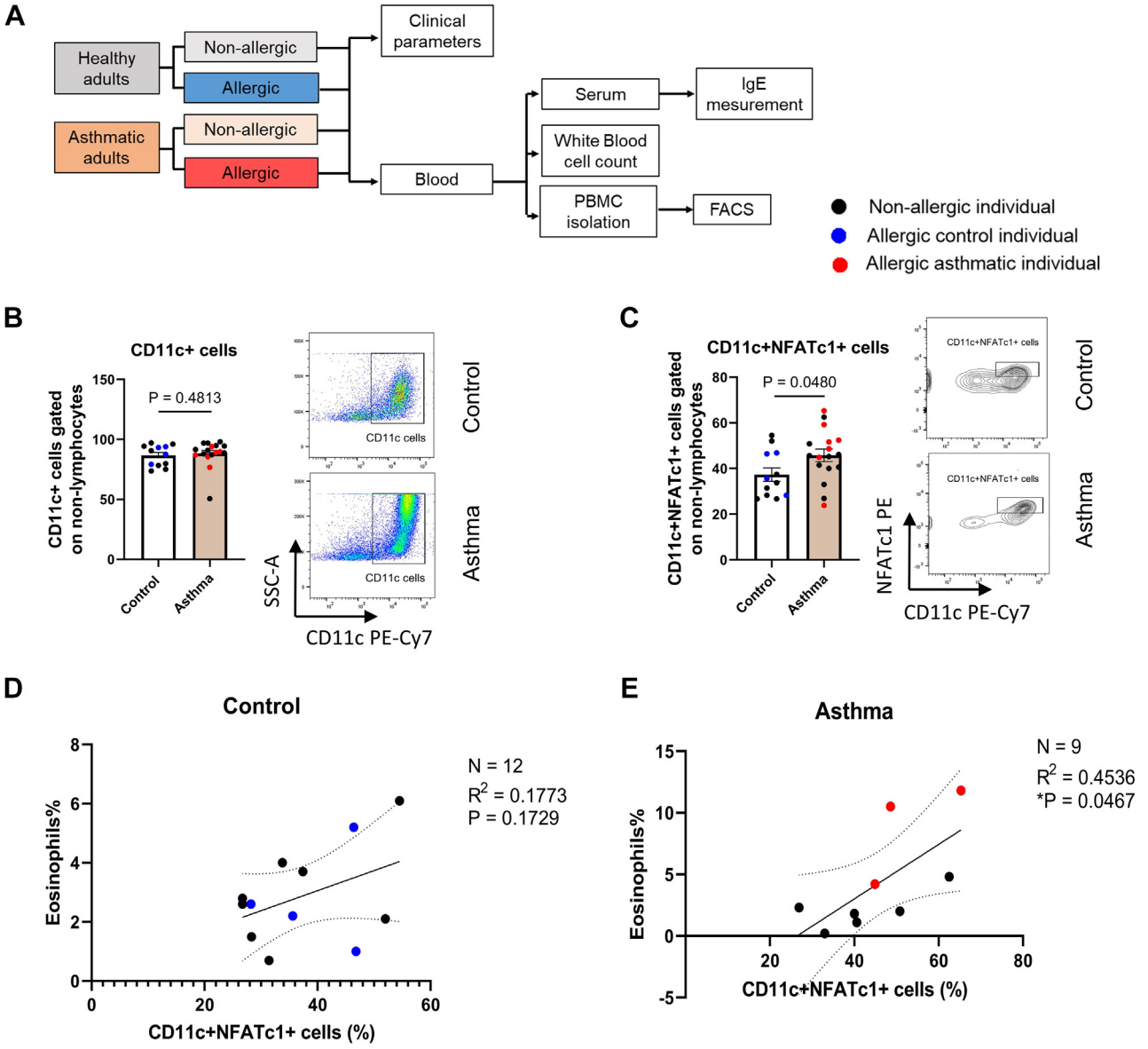

FIG 7. Analysis of $CD11c^+NFATc1^+$ cells and their correlation with eosinophils in AZCRA cohort. **A,** Experimental design showing methodology for AZCRA cohort study. **B,** Flow cytometry analysis shows percentage of $CD11c^+$ cells in control subjects (n = 12) versus asthmatic patients (n = 17). **C,** Percentage of $CD11c^+NFATc1^+$ cells in same groups. Representative dot plots for each group are included. **D** and **E,** Correlation analysis between $CD11c^+NFATc1^+$ cell population and blood eosinophil levels in controls (n = 12) and asthma patients (n = 9) in AZCRA cohort, respectively. Correlations were determined by simple linear regression.

complex, potentially antagonistic relationship between *Nfatc1* and *Foxp3*. Evidence supports the necessity of NFATc1 for FOXP3 expression; however, this relationship appears to evolve, with FOXP3 subsequently acting to inhibit NFATc1.[37-39] Our observations, together with previous research, outline a dynamic and intricate relationship between NFATc1 and Foxp3. Further investigation is needed to fully understand their regulatory mechanisms.

The interaction between IgE and FcεRI, leading to mast cell degranulation, plays a crucial role in the allergic response in asthma.[40] The observed reduction in IgE level and lung mast cells expressing FcεRI in the mice in the absence of *Nfatc1* in T cells suggests a potential attenuation in the allergic phenotype and inflammation.

Our study also explored the role of NFATc1 in DCs in asthma utilizing *Nfatc1*-deficient *Cd11cCre* mice in a HDM-induced model. DCs, crucial in asthma immunity, display elevated MHC molecules and costimulatory proteins during maturation.[41] Downregulation of these proteins' gene expression in *Nfatc1*-deficient CD11c cells suggests that *Nfatc1* absence inhibits this process. Lowered expression of pattern recognition receptors, DC subtype markers, and proinflammatory cytokine expression in *Nfatc1*-deficient CD11c cells suggests impaired pathogen response, maturation, and effector function. The reduced capacity

of these cells to promote T-cell proliferation and the impaired differentiation of BM-derived DCs due to *Nfatc1* deficiency in response to HDM further underscore the critical role of *Nfatc1* in the differentiation and functionality of DCs in the context of asthma. Previous research showed NFAT's key role in DC development and function.[18,42,43] Our data specifically highlight *Nfatc1*'s crucial involvement in DC differentiation in allergic asthma, providing new insights into its impact on immune responses and asthma pathology.

Lung DCs originate from DC progenitors or monocytes in BM.[44] The decrease in the lung DC populations in the *Nfatc1*$^{fl/fl}$ x *Cd11cCre* asthmatic mice aligns with a compromised differentiation process of BM-derived DCs. This reduction of lung DC population may particularly be attributed to decreased CCR7$^+$, CD11b$^+$, and FcεRI$^+$ DC subpopulations. DCs migrate to lymph nodes after allergen exposure to direct T-cell responses in asthma, a process dependent on chemokine receptor CCR7.[25] The significant attenuation in CCR7 expression in the lung DCs of the *Nfatc1*$^{fl/fl}$ x *Cd11cCre* mice implies a compromised migratory capacity of these DCs to the lung-draining lymph nodes. The role of CD11b$^+$, CCR7$^+$, CD40$^+$, and FcεRI$^+$ DC populations has been highlighted in T_H2 cell–mediated immunity in response to allergenic stimuli.[21,22,45,46] Reductions in these DC populations are consistent with the attenuation of T_H2 response in the lung of *Nfatc1*$^{fl/fl}$ x *Cd11cCre* mice.

Additionally, within the HDM-induced asthma model, the attenuation of the T_H2 response is associated with reduced serum total IgE level as well as diminished mast cell and eosinophil populations in the lungs of mice with *Nfatc1* deletion in CD11c$^+$ cells. These phenotypic alterations were accompanied by an improvement in lung function, highlighting the critical role of NFATc1 in CD11c$^+$ cells in modulating allergic and eosinophilic inflammatory processes in asthma. Such evidence underscores the significance of NFATc1 in CD11c cells in the pathophysiology of asthma.

In line with the results from the mouse study, the AZCRA cohort revealed a significant increase in the CD11c$^+$NFATc1$^+$ cell population among asthmatic individuals compared to controls, with a notable correlation to eosinophil counts and percentages. This elevation suggests that the CD11c$^+$NFATc1$^+$ cells likely represent functional DCs critical in orchestrating T_H2-mediated eosinophilic responses in asthma. Furthermore, the correlation underscores the translational significance of our findings, bridging insights from murine models to human asthma research and potentially guiding therapeutic interventions.

Our study has several limitations due to the conditional knockout models, which may inadvertently affect cells beyond the target (eg, CD4$^+$ DCs in *Nfatc1*$^{fl/fl}$ x *Cd4Cre* mice, and other CD11c$^+$ myeloid cells in *Nfatc1*$^{fl/fl}$ x *Cd11cCre* mice). Addressing this requires advanced methods like single-cell RNA-Seq for accurate cell analysis. Additionally, the impact of DCs was detected after intranasal HDM challenge, which raises the possibility that the observed differences in DCs could be influenced by the altered immune environment after challenge. Future studies focusing on the early impact of DCs right after sensitization phase would provide better insights into their role in promoting T-cell differentiation. In future human cohort studies, costaining for GATA3 and FOXP3 in NFATc1$^+$CD4$^+$ cells would provide a more robust validation of our RNA-level findings by directly linking increased NFATc1 expression to specific CD4$^+$ T-cell subsets, such as T_H2 or Treg cells. However, due to ethical and practical constraints, obtaining lung tissue from asthmatic patients was not feasible. As a result, using PBMCs instead of lung tissue presents a limitation in fully capturing the pathophysiologic context of asthma and complicates the translation of findings from mouse models to human disease. In future studies, nasal brushing or lavage and sputum analysis could serve as alternative methods to gain insights into the local immune environment of the lungs. Additionally, *in vitro* coculture strategies involving lung organoids with autologous immune cells offer a viable alternative for studying lung tissue dynamics and immune responses more directly.

In conclusion, our study underscores NFATc1's crucial role in CD4$^+$ T cells and CD11c$^+$ DCs in driving T_H2-mediated eosinophilic inflammation in asthma, suggesting that targeted modulation of NFATc1 in these cells could open new avenues for the development of therapies for allergic asthma, particularly personalized treatments for type 2–high asthma.

DISCLOSURE STATEMENT

Supported by Collaborative Research Centers (SFB) grant CRC1181/TP08 (Checkpoints for Resolution of Inflammation) and a Deutsche Forschungsgemeinschaft (DFG) grant awarded to S.F.

Disclosure of potential conflict of interest: The authors declare that they have no relevant conflicts of interest.

Declaration of generative AI– and AI-assisted technologies in the writing process: During the preparation of this report, the authors used ChatGPT in order to improve readability and language. After using this tool, the authors reviewed and edited the content as needed. The authors take full responsibility for the content of the publication.

We thank L. Glimcher, Weill Cornell University, New York; Chris B. Wilson, University of Washington; and the team at D. Dudziak's laboratory, Friedrich-Alexander-University Erlangen-Nürnberg, Germany, for generously providing the *Nfatc1*$^{fl/fl}$, *Cd4Cre,* and *Cd11cCre* mice, respectively. Special thanks the whole team at the Department of Molecular Pneumology, particularly A. Geiger, E. Nendel, S. Mittler, and S. Trump, for their technical support. We are additionally grateful to Markus F. Neurath, Department of Internal Medicine 1, for helping us with AZCRA cohort recruitment, and C. I. Geppert, Institute of Pathology, Friedrich-Alexander-University Erlangen-Nürnberg, for help with cytospin scans.

Key messages

- **NFATc1 in CD4$^+$ T cells promotes T_H2 cell polarization and enhances their effector functions, influencing type 2–high allergic asthma.**
- **NFATc1 in CD11c$^+$ DCs enhances DC maturation, marked by elevated expression levels of MHC-II, CCR7, FcεRI, and costimulatory proteins, which is essential for T_H2 cell priming in allergic asthma.**
- **NFATc1 in both T cells and DCs promotes T_H2 responses, leading to eosinophil activation, IgE class switching in B cells, and mast cell degranulation, thereby contributing to asthma pathology.**

REFERENCES

1. Hammad H, Lambrecht BN. The basic immunology of asthma. Cell 2021;184:1469-85.

2. Steinke JW, Borish L. Th2 cytokines and asthma. Interleukin-4: its role in the pathogenesis of asthma, and targeting it for asthma treatment with interleukin-4 receptor antagonists. Respir Res 2001;2:66-70.
3. Pelaia C, Paoletti G, Puggioni F, Racca F, Pelaia G, Canonica GW, et al. Interleukin-5 in the pathophysiology of severe asthma. Front Physiol 2019;10:1514.
4. Wills-Karp M. Interleukin-13 in asthma pathogenesis. Immunol Rev 2004;202:175-90.
5. Baine I, Abe BT, Macian F. Regulation of T-cell tolerance by calcium/NFAT signaling. Immunol Rev 2009;231:225-40.
6. Lee M, Park J. Regulation of NFAT activation: a potential therapeutic target for immunosuppression. Mol Cells 2006;22:1-7.
7. Heissmeyer V, Macián F, Im SH, Varma R, Feske S, Venuprasad K, et al. Calcineurin imposes T cell unresponsiveness through targeted proteolysis of signaling proteins. Nat Immunol 2004;5:255-65.
8. Peterson BR, Sun LJ, Verdine GL. A critical arginine residue mediates cooperativity in the contact interface between transcription factors NFAT and AP-1. Proc Natl Acad Sci U S A 1996;93:13671-6.
9. Chen L, Glover JN, Hogan PG, Rao A, Harrison SC. Structure of the DNA-binding domains from NFAT, Fos and Jun bound specifically to DNA. Nature 1998;392(6671):42-8.
10. Chuvpilo S, Jankevics E, Tyrsin D, Akimzhanov A, Moroz D, Jha MK, et al. Autoregulation of *NFATc1/A* expression facilitates effector T cells to escape from rapid apoptosis. Immunity 2002;16:881-95.
11. Serfling E, Avots A, Klein-Hessling S, Rudolf R, Vaeth M, Berberich-Siebelt F. *NFATc1*/αA: the other face of NFAT factors in lymphocytes. Cell Commun Signal 2012;10:16.
12. Koch S, Knipfer L, Kölle J, Mirzakhani H, Graser A, Zimmermann T, et al. Targeted deletion of NFAT-interacting-protein-(NIP) 45 resolves experimental asthma by inhibiting innate lymphoid cells group 2 (ILC2). Sci Rep 2019;9:15695.
13. Koch S, Graser A, Mirzakhani H, Zimmermann T, Melichar VO, Wölfel M, et al. Increased expression of nuclear factor of activated T cells 1 drives IL-9–mediated allergic asthma. J Allergy Clin Immunol 2016;137:1898-902.e7.
14. Koch S, Reppert S, Finotto S. *NFATc1* deletion in T lymphocytes inhibits the allergic trait in a murine model of asthma. Clin Exp Allergy 2015;45:1356-66.
15. Goodridge HS, Simmons RM, Underhill DM. Dectin-1 stimulation by *Candida albicans* yeast or zymosan triggers NFAT activation in macrophages and dendritic cells. J Immunol 2007;178:3107-15.
16. Zanoni I, Ostuni R, Capuano G, Collini M, Caccia M, Ronchi AE, et al. CD14 regulates the dendritic cell life cycle after LPS exposure through NFAT activation. Nature 2009;460(7252):264-8.
17. Khameneh HJ, Ho AW, Spreafico R, Derks H, Quek HQ, Mortellaro A. The Syk–NFAT–IL-2 pathway in dendritic cells is required for optimal sterile immunity elicited by alum adjuvants. J Immunol 2017;198:196-204.
18. Kayama H, Koga R, Atarashi K, Okuyama M, Kimura T, Mak TW, et al. *NFATc1* mediates Toll-like receptor–independent innate immune responses during *Trypanosoma cruzi* infection. PLoS Pathog 2009;5:e1000514.
19. Herbst S, Shah A, Mazon Moya M, Marzola V, Jensen B, Reed A, et al. Phagocytosis-dependent activation of a TLR9–BTK–calcineurin–NFAT pathway co-ordinates innate immunity to *Aspergillus fumigatus*. EMBO Mol Med 2015;7:240-58.
20. Li N, Mirzakhani H, Kiefer A, Koelle J, Vuorinen T, Rauh M, et al. Regulated on activation, normal T cell expressed and secreted (RANTES) drives the resolution of allergic asthma. iScience 2021;24:103163.
21. Plantinga M, Guilliams M, Vanheerswynghels M, Deswarte K, Branco-Madeira F, Toussaint W, et al. Conventional and monocyte-derived CD11b^{+} dendritic cells initiate and maintain T helper 2 cell–mediated immunity to house dust mite allergen. Immunity 2013;38:322-35.
22. Hammad H, Lambrecht BN, Pochard P, Gosset P, Marquillies P, Tonnel AB, et al. Monocyte-derived dendritic cells induce a house dust mite–specific Th2 allergic inflammation in the lung of humanized SCID mice: involvement of CCR7. J Immunol 2002;169:1524-34.
23. Hintzen G, Ohl L, del Rio ML, Rodriguez-Barbosa JI, Pabst O, Kocks JR, et al. Induction of tolerance to innocuous inhaled antigen relies on a CCR7-dependent dendritic cell–mediated antigen transport to the bronchial lymph node. J Immunol 2006;177:7346-54.
24. Hock M, Vaeth M, Rudolf R, Patra AK, Pham DA, Muhammad K, et al. *NFATc1* induction in peripheral T and B lymphocytes. J Immunol 2013;190:2345-53.
25. Pan M, Winslow MM, Chen L, Kuo A, Felsher D, Crabtree GR. Enhanced *NFATc1* nuclear occupancy causes T cell activation independent of CD28 costimulation. J Immunol 2007;178:4315-21.
26. Yamashita M, Ukai-Tadenuma M, Miyamoto T, Sugaya K, Hosokawa H, Hasegawa A, et al. Essential role of GATA3 for the maintenance of type 2 helper T (Th2) cytokine production and chromatin remodeling at the Th2 cytokine gene loci. J Biol Chem 2004;279:26983-90.
27. Sasaki T, Onodera A, Hosokawa H, Watanabe Y, Horiuchi S, Yamashita J, et al. Genome-wide gene expression profiling revealed a critical role for GATA3 in the maintenance of the Th2 cell identity. PLoS One 2013;8:e66468.
28. Shoemaker J, Saraiva M, O'Garra A. GATA-3 directly remodels the IL-10 locus independently of IL-4 in CD4^{+} T cells. J Immunol 2006;176:3470-9.
29. Klein-Hessling S, Bopp T, Jha MK, Schmidt A, Miyatake S, Schmitt E, et al. Cyclic AMP-induced chromatin changes support the NFATc-mediated recruitment of GATA-3 to the interleukin 5 promoter. J Biol Chem 2008;283:31030-7.
30. So T, Song J, Sugie K, Altman A, Croft M. Signals from OX40 regulate nuclear factor of activated T cells c1 and T cell helper 2 lineage commitment. Proc Natl Acad Sci U S A 2006;103:3740-5.
31. Yoshida H, Nishina H, Takimoto H, Marengère LE, Wakeham AC, Bouchard D, et al. The transcription factor NF-ATc1 regulates lymphocyte proliferation and Th2 cytokine production. Immunity 1998;8:115-24.
32. Nobs SP, Natali S, Pohlmeier L, Okreglicka K, Schneider C, Kurrer M, et al. PPARγ in dendritic cells and T cells drives pathogenic type-2 effector responses in lung inflammation. J Exp Med 2017;214:3015-35.
33. Morimoto Y, Hirahara K, Kiuchi M, Wada T, Ichikawa T, Kanno T, et al. Amphiregulin-producing pathogenic memory T helper 2 cells instruct eosinophils to secrete osteopontin and facilitate airway fibrosis. Immunity 2018;49:134-50.e6.
34. Mesnil C, Raulier S, Paulissen G, Xiao X, Birrell MA, Pirottin D, et al. Lung-resident eosinophils represent a distinct regulatory eosinophil subset. J Clin Invest 2016;126:3279-95.
35. Novosad J, Krčmová I, Souček O, Drahošová M, Sedlák V, Kulířová M, et al. Subsets of eosinophils in asthma, a challenge for precise treatment. Int J Mol Sci 2023;24:5716.
36. Diehl S, Krahl T, Rinaldi L, Norton R, Irvin CG, Rincón M. Inhibition of NFAT specifically in T cells prevents allergic pulmonary inflammation. J Immunol 2004;172:3597-603.
37. Tone Y, Furuuchi K, Kojima Y, Tykocinski ML, Greene MI, Tone M. Smad3 and NFAT cooperate to induce *Foxp3* expression through its enhancer. Nat Immunol 2008;9:194-202.
38. Li X, Liang Y, LeBlanc M, Benner C, Zheng Y. Function of a Foxp3 *cis*-element in protecting regulatory T cell identity. Cell 2014;158:734-48.
39. Torgerson TR, Genin A, Chen C, Zhang M, Zhou B, Añover-Sombke S, et al. FOXP3 inhibits activation-induced *NFAT2* expression in T cells thereby limiting effector cytokine expression. J Immunol 2009;183:907-15.
40. Janeway CA Jr, Travers P, Walport M, Shlomchik MJ. Effector mechanisms in allergic reactions. New York: Garland Science; 2001.
41. Dalod M, Chelbi R, Malissen B, Lawrence T. Dendritic cell maturation: functional specialization through signaling specificity and transcriptional programming. EMBO J 2014;33:1104-16.
42. Matsue H, Yang C, Matsue K, Edelbaum D, Mummert M, Takashima A. Contrasting impacts of immunosuppressive agents (rapamycin, FK506, cyclosporin A, and dexamethasone) on bidirectional dendritic cell-T cell interaction during antigen presentation. J Immunol 2002;169:3555-64.
43. Tajima K, Amakawa R, Ito T, Miyaji M, Takebayashi M, Fukuhara S. Immunomodulatory effects of cyclosporin A on human peripheral blood dendritic cell subsets. Immunology 2003;108:321-8.
44. van Rijt LS, Prins JB, Leenen PJ, Thielemans K, de Vries VC, Hoogsteden HC, et al. Allergen-induced accumulation of airway dendritic cells is supported by an increase in CD31^{hi}Ly-6C^{-} bone marrow precursors in a mouse model of asthma. Blood 2002;100:3663-71.
45. Díaz Á, González-Alayón I, Pérez-Torrado V, Suárez-Martins M. CD40-CD154: a perspective from type 2 immunity. Semin Immunol 2021;53:101528.
46. Sallmann E, Reininger B, Brandt S, Duschek N, Hoflehner E, Garner-Spitzer E, et al. High-affinity IgE receptors on dendritic cells exacerbate Th2-dependent inflammation. J Immunol 2011;187:164-71.